ER-5386

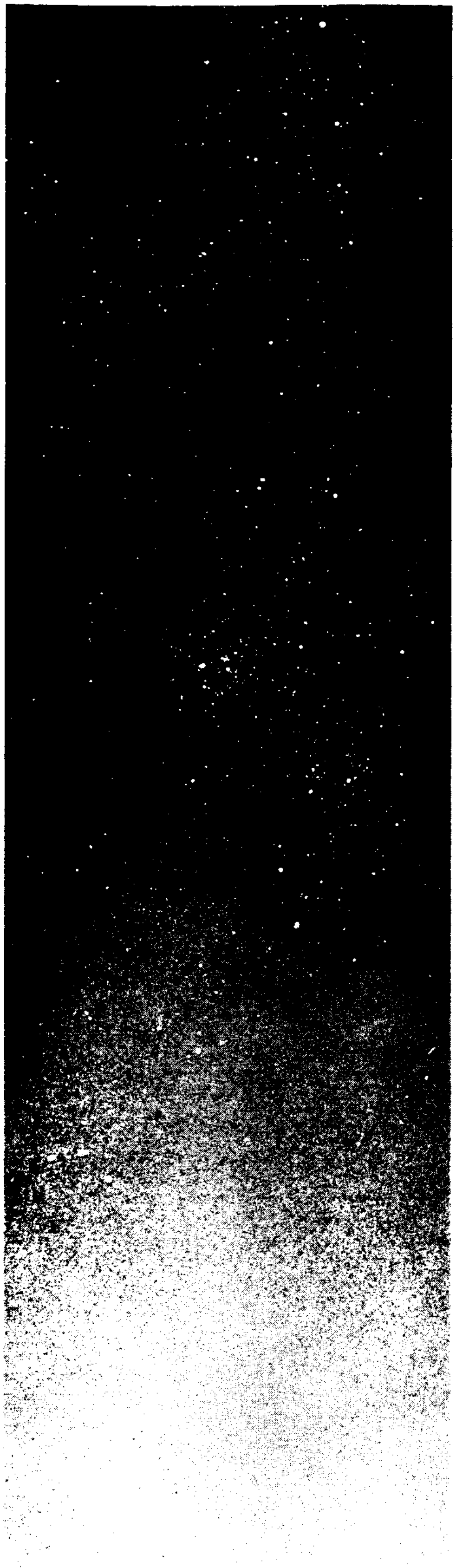

SUNFLOWER POWER CONVERSION SYSTEM

QUARTERLY REPORT

Technical Management
NASA-Lewis Research Center
Aux. Power Generating Office
Attn.: J. A. Heller (86-1)

MARCH 1963 – MAY 1963

TAPCO a division of
Thompson Ramo Wooldridge Inc.

NOTICE

TABLE OF CONTENTS

LIST OF ILLUSTRATIONS

1. PROJECT OBJECTIVES

The Sunflower program objectives are to accomplish fabrication, test, and development tasks oriented toward confirming the conceptual validity and performance feasibility of a solar-powered 3 Kw mercury Rankine power conversion system. Major items include solution to long-term, high temperature lithium hydride containment, demonstration of component operation and endurance integrity, experimental confirmation of the design integrity of the aluminum honeycomb petaline collector, and operational integrity of the integrated Rankine system.

II. PROJECT OBJECTIVES FOR THE REPORTING PERIOD OF MARCH 1, 1963 THROUGH JUNE 1, 1963

Performance and endurance testing of turbo-alternator units 1-3A, 1-1B, and 1-4 will be scheduled depending upon utilization of the test rig.

Full scale solar collector vibration testing will be completed.

Operation of the workhorse loop will be continued and will be directed at determining the hydrogen removal capabilities of the existing plumbing, hydrogen windows, and centrifugal separators.

In addition, testing of the hydrogen swallowing capabilities of the jet centrifugal pump will be reinitiated.

The forced circulation mercury corrosion loop testing will be continued toward the 5000 hour objectives.

Additional work will be continued on completion of the Boiler/Heat Storage, Solar Collector, and Condenser Subcooler Topical Report.

III. PROJECT PROGRESS DURING THE REPORTING PERIOD

PROJECT MANAGEMENT

During the reporting period, numerous conversations and meetings were conducted with NASA regarding the redirection of system testing as affected by the operation of the condenser. As of this time, the results of these discussions have lead to the holding in abeyance of any further system testing until questions resolving applicability of the $\pm$ 1 "g" specification to flight missions is evaluated. This specification greatly influences condenser performance and operation of the system in the ground environment. Further system testing will depend on resolution of these specifications consistent with the objectives of NASA's 1964 FY planning.

Test plans for turbo-alternator testing, completion of CSU I-3 analysis work and test reports for this unit were prepared.

Data reduction and analysis has continued on a full time basis, reducing data for the CSU I-3A endurance test run. In addition to CSU testing, work has been performed in the evaluation of test results of the vibration testing of the full scale solar collector.

TEST RIG DESIGN AND FABRICATION

Component test rig activities during the quarter have been conducted in support of turbo-alternator testing. CSU I-3A testing was continued on endurance test objectives for 768 hours. At this time, step changes in power output were observed which were believed to have been caused by foreign particles entering the first stage turbine nozzle of the turbo-alternator unit. The unit was voluntarily shut down and the turbine housing examined. The nozzle passages were restricted by particles approximately 40-60 thousandths of an inch in dimension and of irregular shape. The particles were removed from the turbine housing, the unit reassembled, and the endurance test continued. During this shutdown, modifications of the test rig were incorporated in an attempt to stop the formation of deposits which could cause small particles to form and be carried down stream to the turbine housing.

The rig modifications are shown schematically in Figures 1 and 2. These show the rig during the 768 hour test and then the modified rig prior to resumption of testing. The changes that occured were:

1. Removal of metering and shut-off valves from the position immediately upstream of the turbine to a location at the exit of the boiler prior to the superheater. This is done primarily for two reasons:

   a. lowering of the operating temperature.

   b. observations of the condition of a similar type valve at this location.

SCHEMATIC - SUNFLOWER TEST RIG

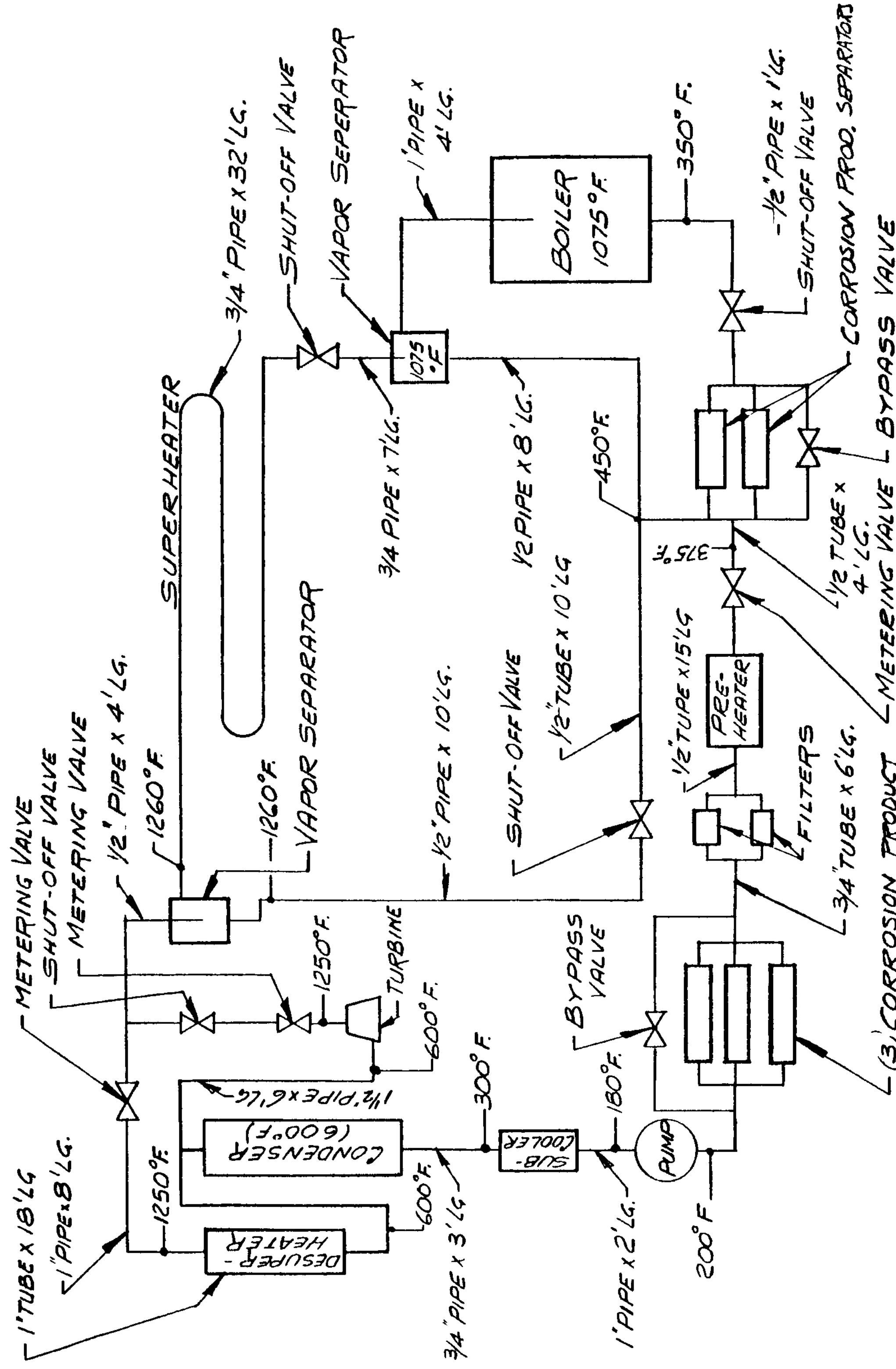

FIGURE 1

SCHEMATIC - SUNFLOWER TEST RIG MODIFICATIONS AFTER 768 HOUR TEST

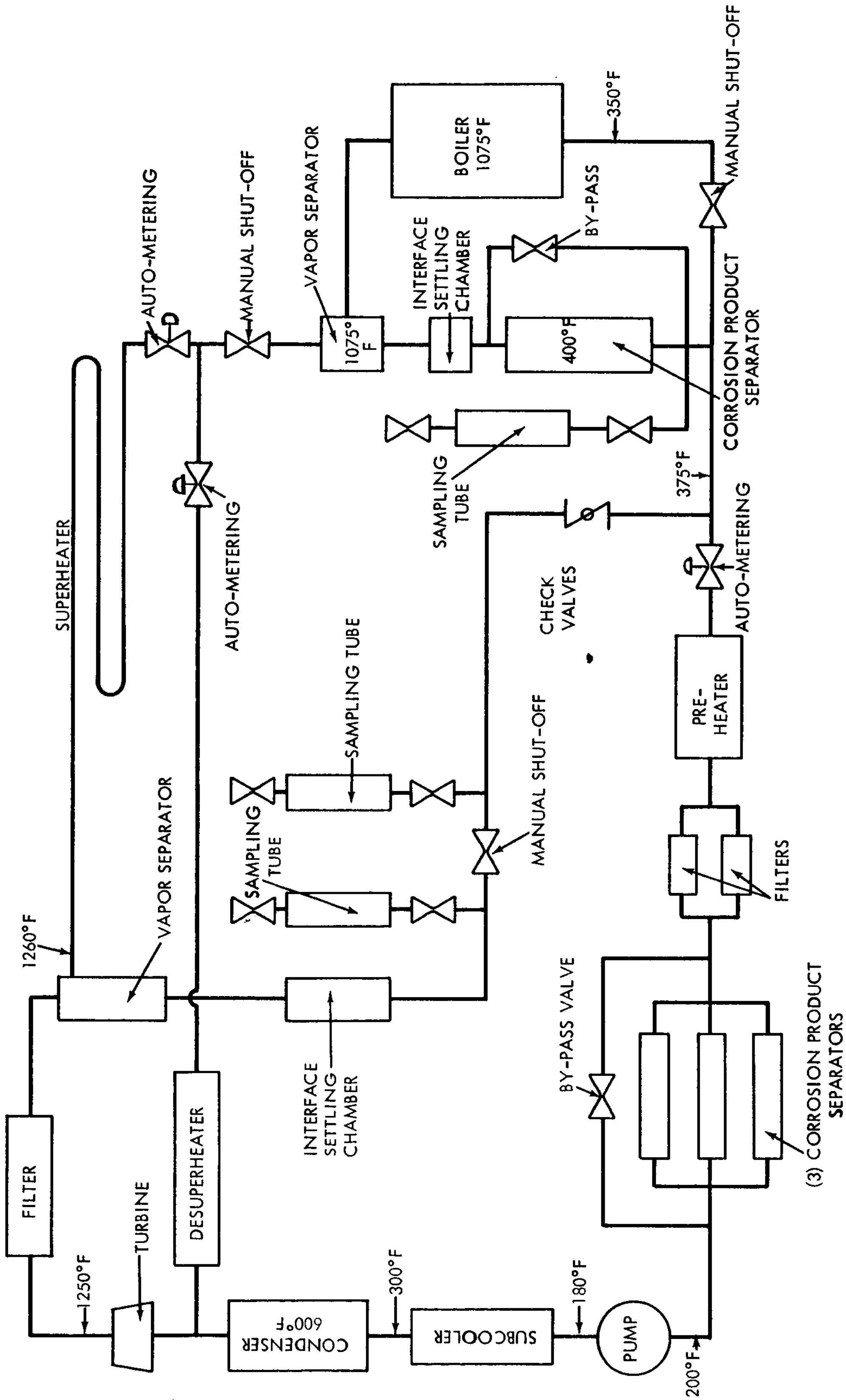

FIGURE 2

2. Placement of the by-pass function of the test rig to a similar location.

3. Use of a shut-off valve rather than a metering valve at the turbine inlet. This increases the flow restriction size and is identical to the valve which has shown good service at this location for a period of approximately 4000 hours.

4. Movement of the location of the centrifugal separator to a position immediately in front of the turbine and insulation of the liquid drain line from the separator to the interface. This reduces the rate of condensation occurring in this line.

5. Removal of the present corrosion product separator at the boiler inlet and insertion of a single corrosion product separator insulated in the liquid return of the boiler centrifugal separator. This allows operation at temperatures of approximately 600°F to determine whether the corrosion product separator is functioning properly.

6. Addition of a check valve in the superheater centrifugal separator return line to prevent inadvertent back flow of fluid toward the turbine in the event of an emergency or normal shut down.

7. Incorporation of collector pots in various locations in the rig to determine whether corrosion products carried in the flow stream have a tendency to rise in vertical lines and to allow trapping of these products. These collector pots may be removed from the rig without affecting rig operation and can be periodically inspected to determine whether the trapping of products in this manner is successful.

An inline filter will be tested as part of the test rig check out for possible use as a filtering element immediately in front of the turbine inlet housing, the purpose being to catch or restrict foreign particles.

SOLAR COLLECTOR

Testing of the fullscale 32 ft. preprototype solar collector was completed in both the stowed and deployed configurations on the MB-C-210 vibration equipment. Figure 3 shows the installation of the simulated PCS structure, collector mounting ring and associated vibration test equipment prior to installation of the solar collector panels. Figure 4 shows the test configurations of the collector with the vibration fixture, simulated structure, and collector installed on the shaker.

Initial testsinvolved conducting a low "g" level survey across the entire spectrum to determine resonant points and possible areas of amplification of the "g" level. This test was conducted at 1/4 "g" between the limits of 5 and 2,000 cps. In the stowed position, two resonant points of concern were noted at approximately 30 and 175 cps. After this survey

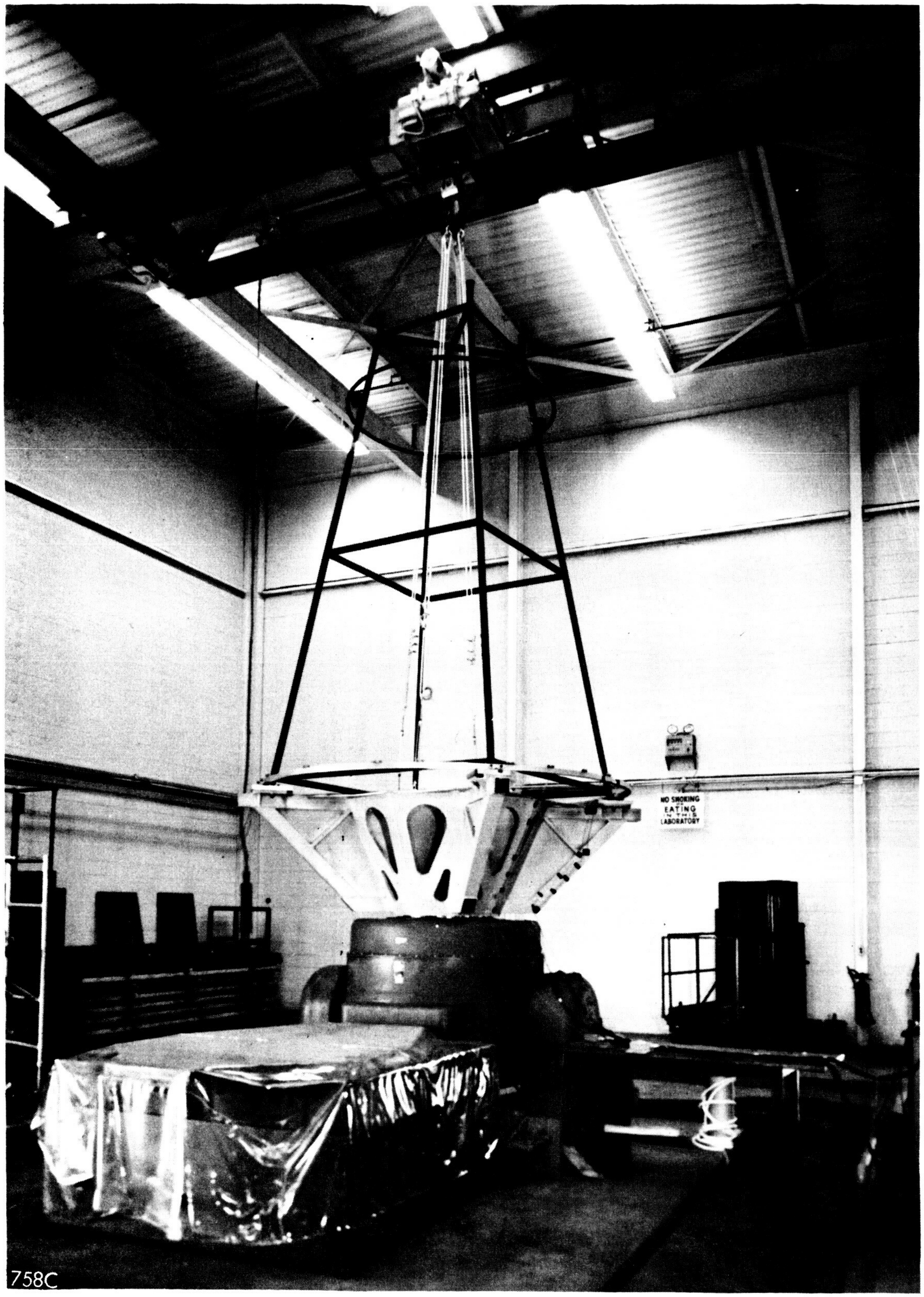

SUNFLOWER VIBRATION TEST FIXTURE AND COLLECTOR SUPPORT
ON C-210 SHAKER

FIGURE 3

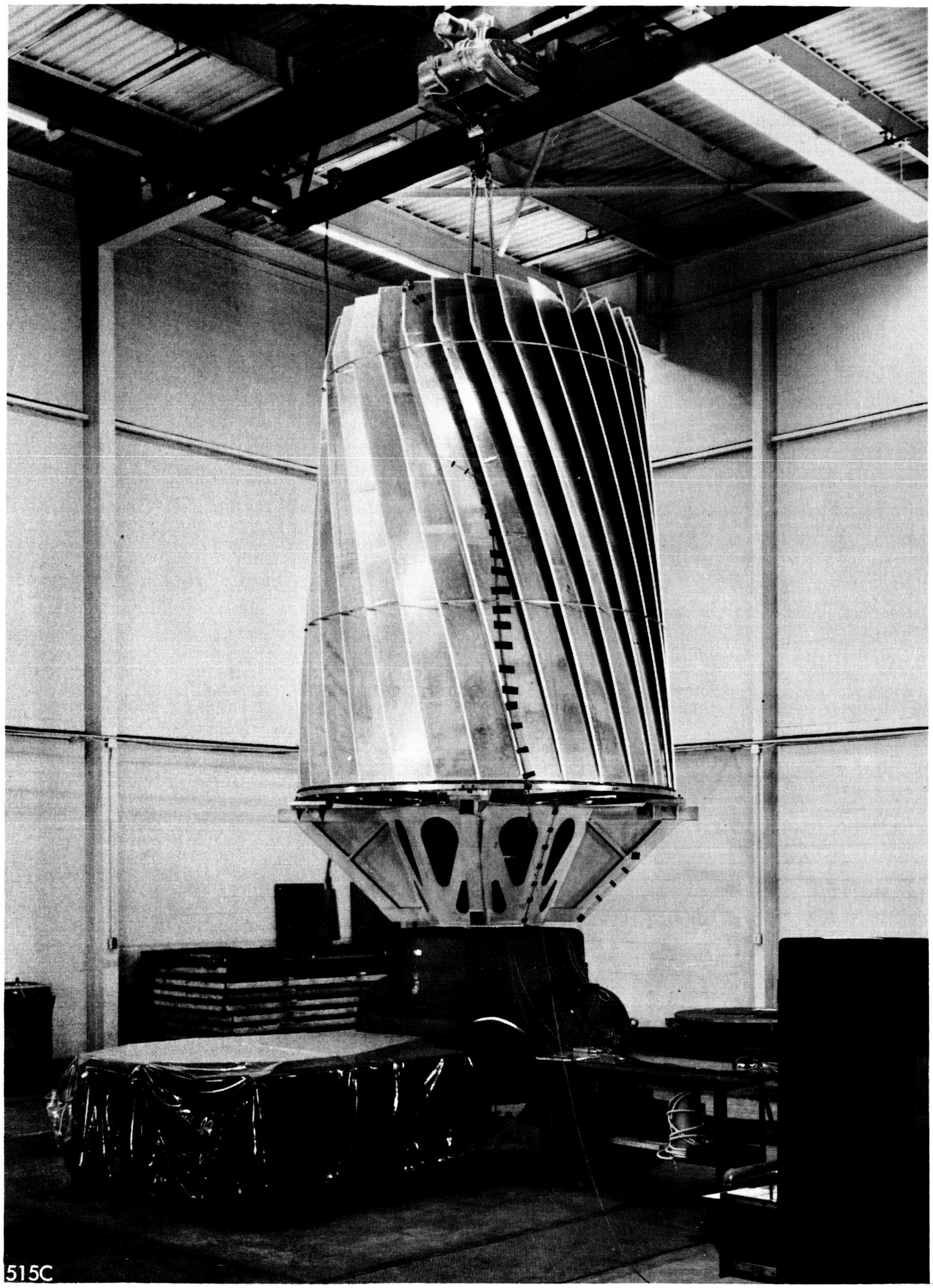

COLLECTOR VIBRATION TEST INSTALLATION

FIGURE 4

was completed, the "g" level was raised and a similar survey conducted. Again the two resonant points appeared and showed "g" levels higher than the input of the shaker exciter table. These resonances occur when either of two factors are noted:

a. When the vibration isolators due to "g" levels imposed, bottom from high loading in the amplified "g" field and do not transmit reduced forces.

b. When the vibration exciter accelerometer control points become difficult to monitor with the existing equipment and allow the set point "g" level to change due to resonance coupled with cross axis vibration and general feed back into the shaker controller.

Figure 5 shows the results of the stowed vibration testing of the full scale 32' solar collector as testing was continued. Two points at 30 and 175 cps were manually reduced in "g" level to prevent excessive "g's" from appearing on the collector and consequently to prevent possible structural damage. Although the maximum "g" level which the collector can withstand is not known, it was felt that the panels should not exceed an input of 10 "g's".

The collector was visually inspected for vibration damage and was found to be free of vibration induced damaged areas.

The collector was then opened on the vibration exciter and similar vibration survey and "g" level tests were conducted in the deployed position.

Figures 6 and 7 show the test arrangement prior to open vibration testing. During the low level "g" survey of the collector in this position (at a "g" level of 2 "g's" and frequency of 13 cps), a midspan fastener failed on one of the panels. After stopping the test, the panel and fastener were examined and found to be improperly bonded into the honeycomb core. The panel was repaired and placed back in the assembly for additional testing. Low level survey was conducted through the same "g" levels and frequencies at which the pullout of the fastener occured with no incident, confirming that the fastener was improperly bonded.

The deployed vibration test also had the objective of subjecting the open collector to a vibration spectrum of 5 to 2,000 cycles/sec with "g" levels from 0.8 to 7.5 "g's". Although the specification is quite severe for orbital transfer maneuvers, the collector was evaluated throughout the entire frequency range. Figure 8 shows the results of the vibration testing of the solar collector in the deployed position. As can be noted, two or three resident points were again reduced in "g" level in order to complete the full spectrum without exceeding the 10 "g" limit on the panel surface.

The collector was removed from the vibration test area and reassembled for optical inspection. The final optical inspection is completed and has shown that negligible damage occurred. The existing damage occurred during a high "g" level input near a torsion bar device and resulted in the added peeling of the skin where previous damage had been experienced.

SUNFLOWER COLLECTOR STOWED VIBRATION
TEST RESULTS
(DATA COMPILED FROM 16 TESTS)

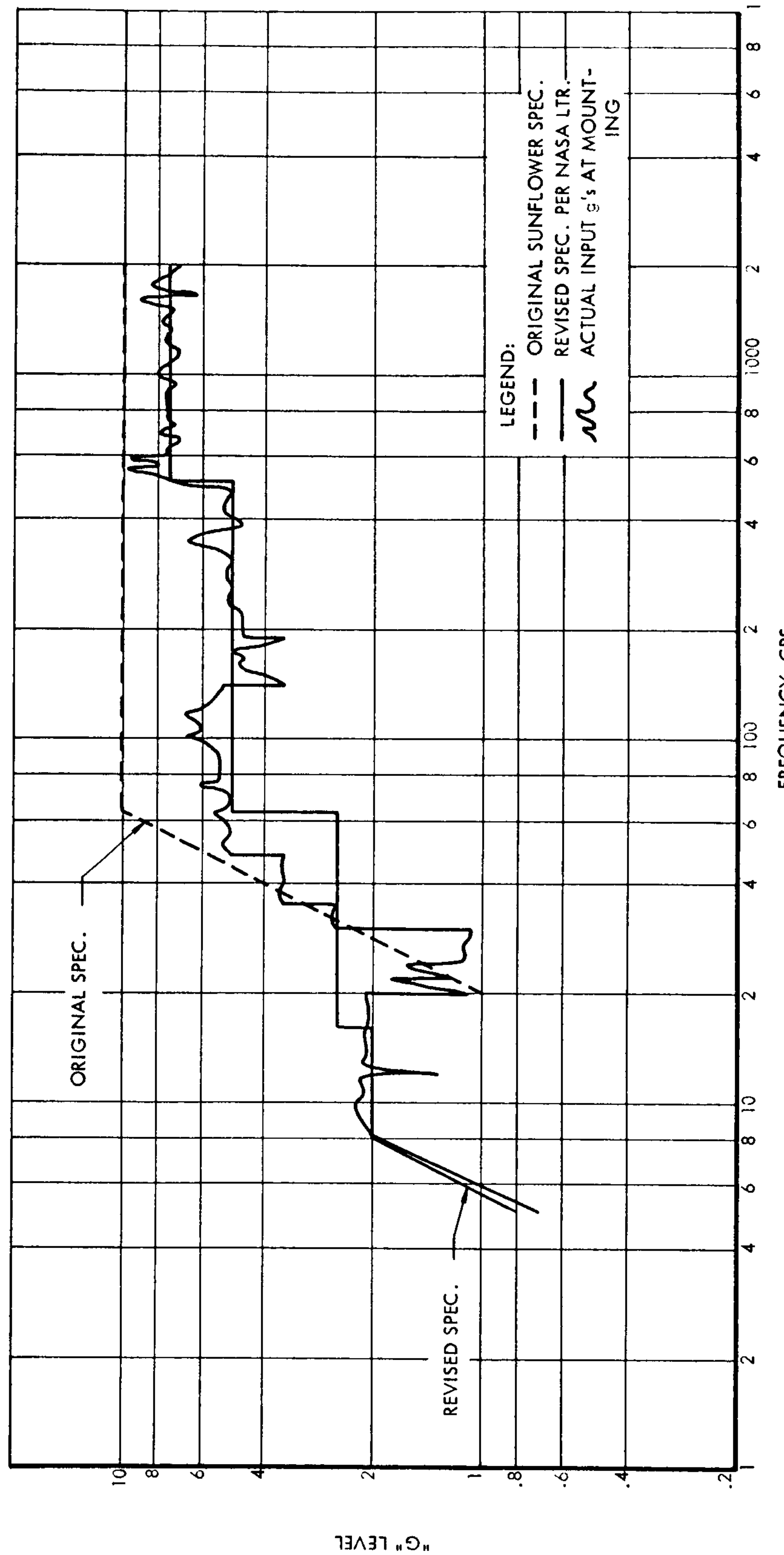

FIGURE 5

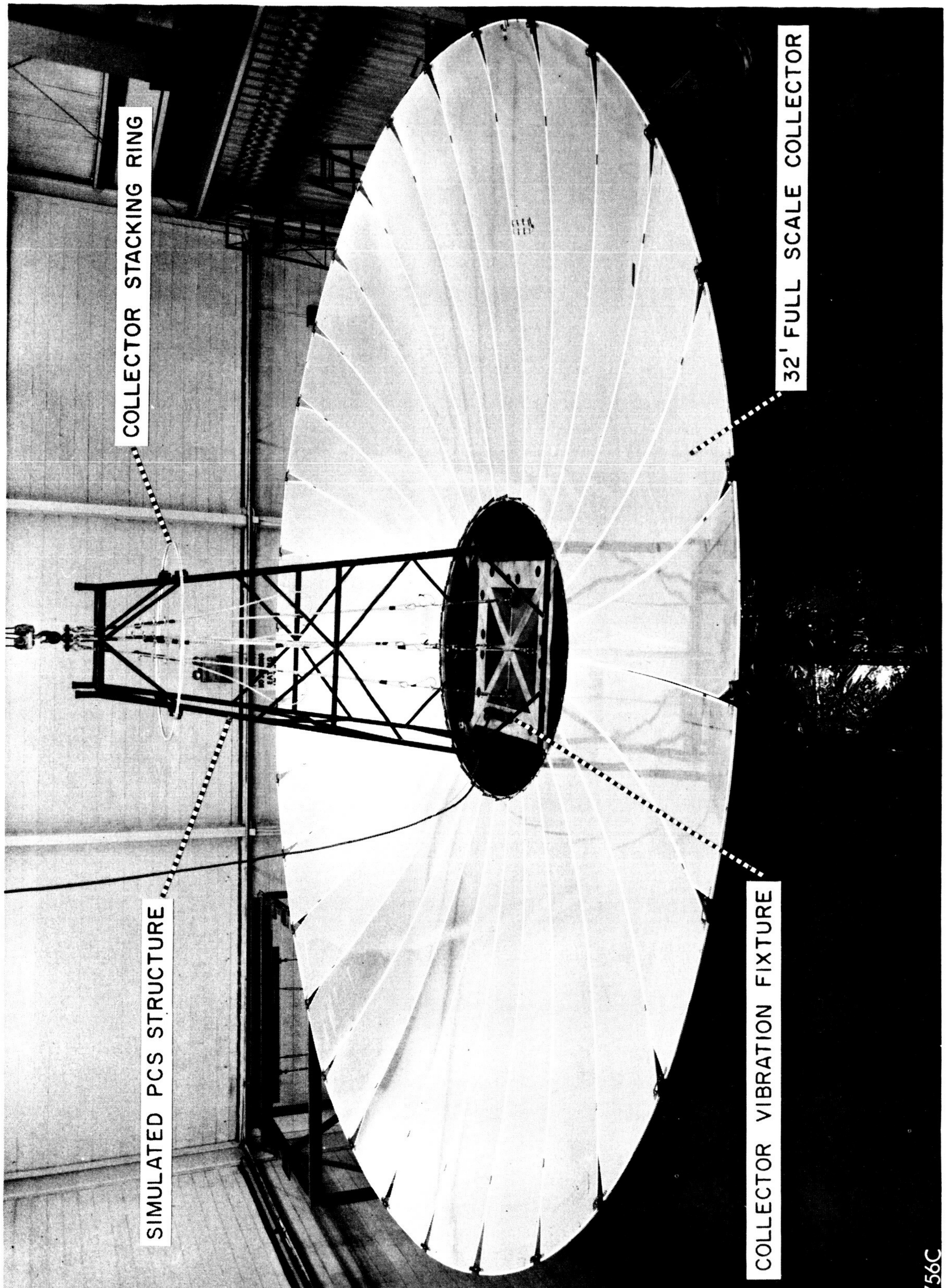

DEPLOYED COLLECTOR VIBRATION TEST INSTALLATION

FIGURE 6

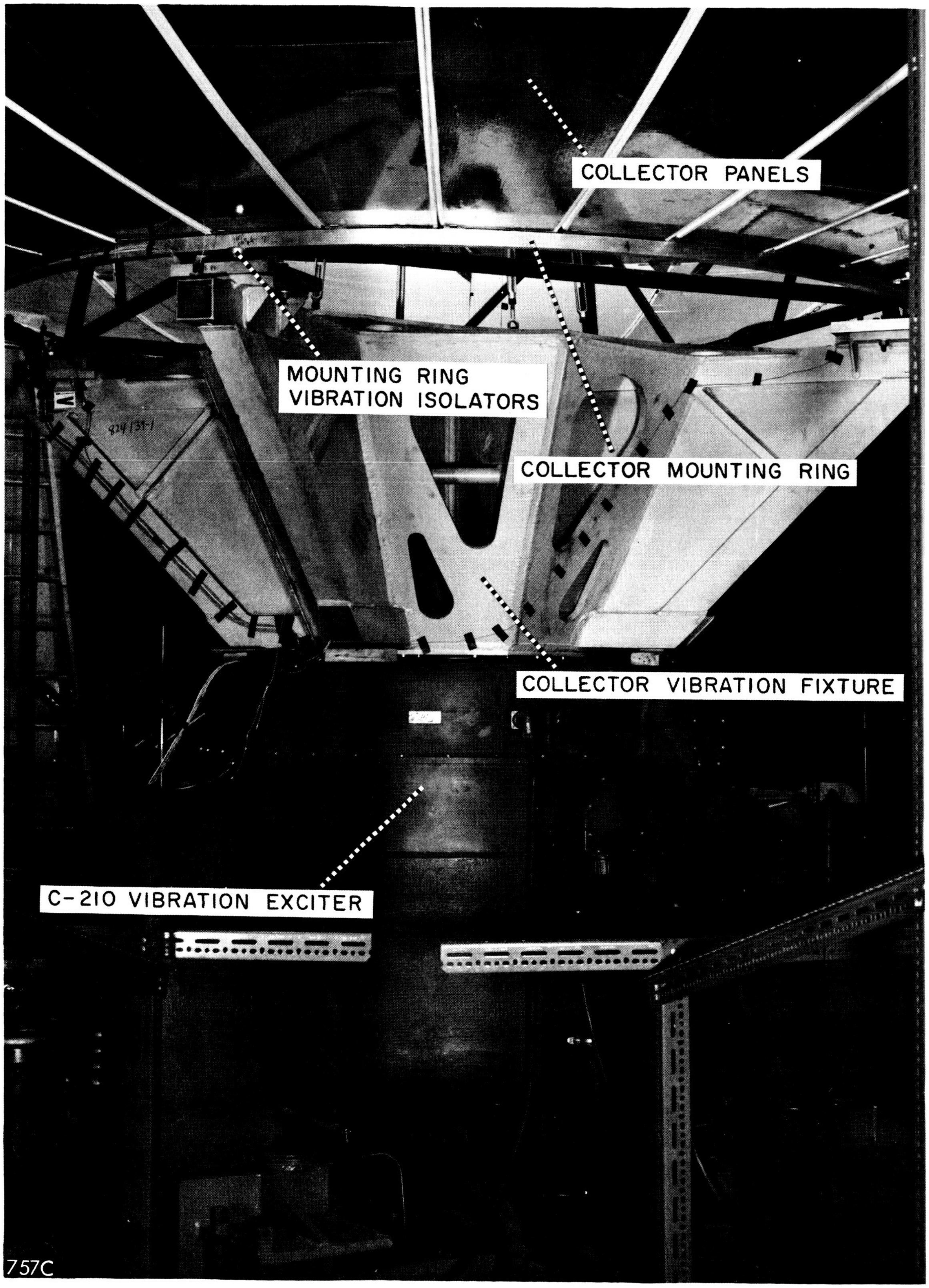

DEPLOYED COLLECTOR VIBRATION TEST INSTALLATION, BOTTOM VIEW

FIGURE 4

SUNFLOWER COLLECTOR DEPLOYED VIBRATION
TEST RESULTS
(DATA COMPILED FROM 16 TESTS)

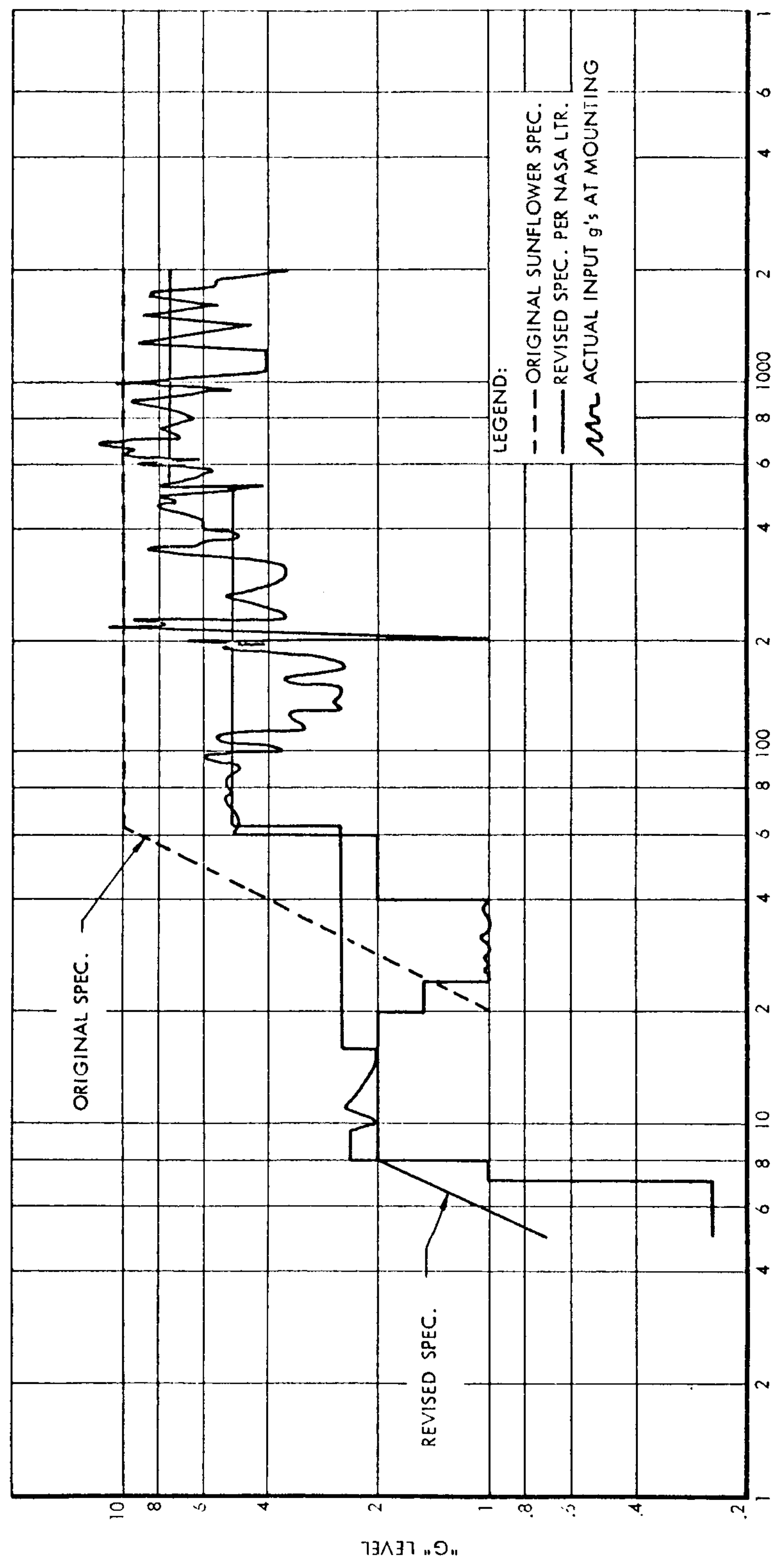

FIGURE 8

The results are encouraging since the collector withstood much higher "g" levels than would be experienced in the flight version. The minimal damage that did occur was contributed to peeling of already damaged areas due to handling, etc. The results illustrate that with surfaces which are completely bonded with no peel areas, the solar collector should be more than adequate in its present form to meet environmental launch and deployed vibration specifications.

Preparation of the Solar Collector Topical Report, which will cover all aspects of the solar collector activity conducted on the Sunflower program, was continued. This report is expected to be completed during the next quarter.

TURBO-ALTERNATOR

Turbo-alternator CSU I-3A accumulated 768 hours of continuous endurance testing before being voluntarily shut down when foreign particles entered the first stage nozzle from the component test rig. During the last few hours of operation, step changes in power output were observed with subsequent reduction of flow in the test rig. The frequency to which the step changes occurred increased with time and the unit was therefore voluntarily shut down. Post test examinations of the turbine inlet housing, combined with the actual operating conditions of the unit, suggested that particles sufficiently large to block the throat area of the first stage nozzle had entered the turbine housing. This has been confirmed. Figure 9 shows a random sampling of particles removed from the first stage nozzle. This phenomena had not been seen previously in operation of any other units.

Subsequent review of the test rig data indicates that a shut down of the test rig prior to installation and initiation of CSU I-3A test resulted in back flowing mercury from the boiler, up through a centrifugal separator, into the discharge of the superheater, and to an area in front of the metering and shut-off valves at the CSU turbine inlet. These two valves revealed two distinct types of corrosion product deposition. The metering valve located in front of the turbine nozzle showed a very definite vapor deposition of products in a thin layer on the stem of the metering valve. The emergency shut-off valve, however, experienced corrosion products which are believed to have been formed by corrosion products floating on the surface of the mercury during this inadvertent back flush, with subsequent evaporation of the mercury leaving the relatively hard chrome and nickel deposits which were observed. Subsequent operation of the test rig with the CSU then eroded and dislodged portions of these deposits, which were carried down stream into the turbine housing. This caused the step changes in power. As a result of the formation of these particles, several changes in the concept of the test rig have been incorporated. These attempt to prohibit the formation of products on the metering shut-off valves and to include a filter in the turbine inlet line to prevent passage of this size of particles through the plumbing into the unit. These details are explained more fully in the test rig section of the report.

What kind?

The unit was reinstalled in the test rig on April 16 and has been successfully operated throughout the remainder of the quarter and up through the writing of this report. The unit in both tests has accumulated in excess of 2300 hours of operation, its performance being excellent. The alternator and thrust bearing stationary members have been in both the

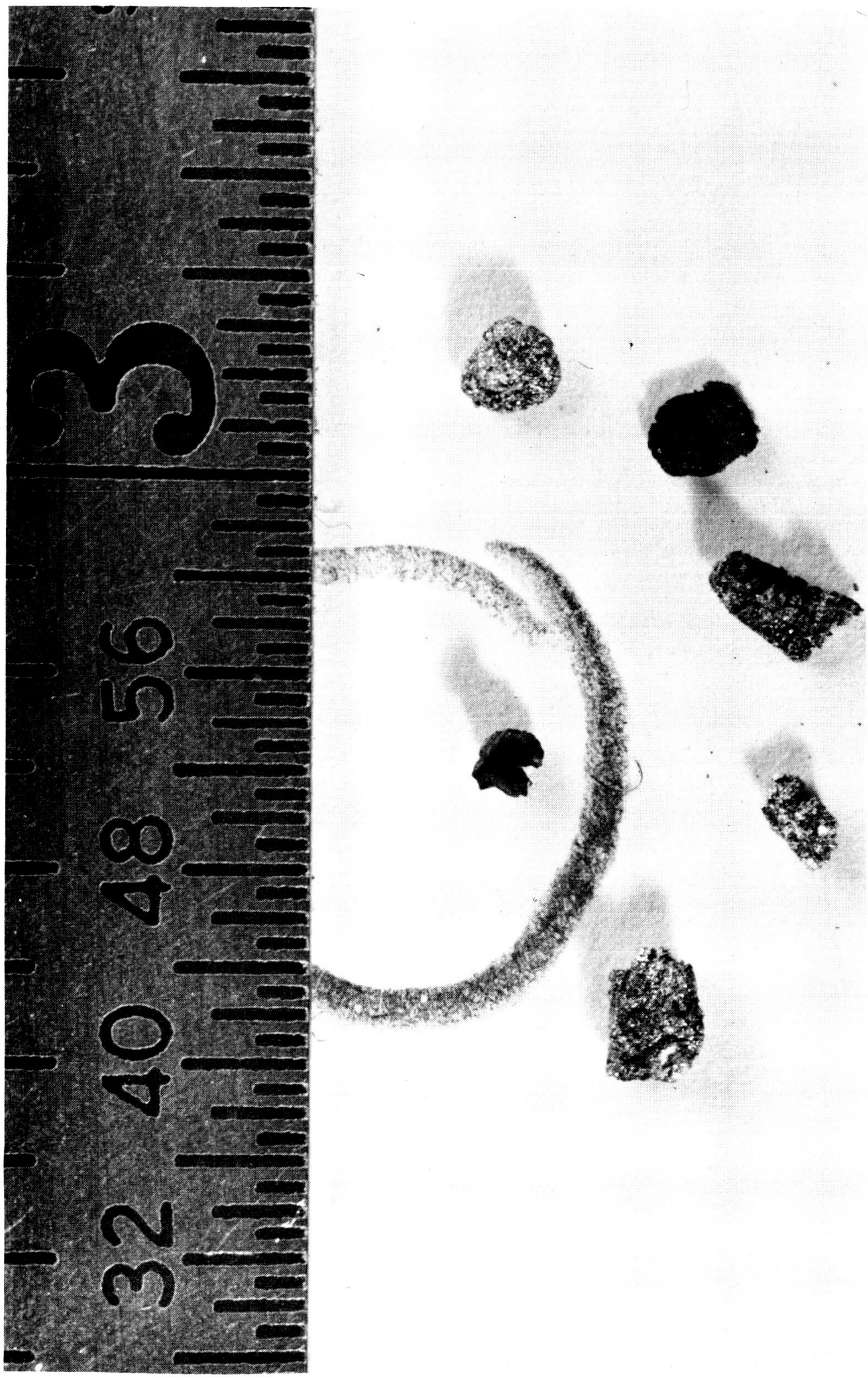

PARTICLES LODGED IN CSU I-3A TURBINE HOUSING

FIGURE 9

CROLOY 9M

SOLARAMIC COATED CROLOY 9M.

HAYNES #25 COATED WITH MO-SI COATING.

TUNGSTEN

TITANIUM COATED HAYNES #25

VANAD COATED 304 STAINLESS STEEL.

CSU I-3 and CSU I-3A testing and have to date accumulated 4678 hours of operation.

Some of the data which have been accumulated to date are tabulated in Table I. These data are tested under two categories, endurance and performance.

In the endurance test data, the mean values represent the nominal design temperature, pressure, flow, etc., while the maximum and minimum values indicate the variations which have occurred during the entire 2300 hour test of this unit. Comparison of the data shows the extremely steady state conditions which prevail during this type of testing.

The performance test data, on the other hand, describes briefly the excursions which turbo-alternators have been purposely exposed to in order to evaluate sensitivity to operating conditions. These values are not the limits of the machine, but only the limits to which off-design testing has thus far been conducted.

No unit has experienced failure from any of these operating parameters. The results are impressive and show the basic design integrity and ability of the unit to perform throughout many off-design conditions.

Lithium Hydrogen Containment

Continued hydrogen permeability measurements have been made during the reporting period and include the following samples:

1. Evaluation of the permeability of hydrogen through Croloy 9M material.
2. Evaluation of the permeability of hydrogen through a solaramic coated Croloy 9M sample.
3. Evaluation of the permeability of hydrogen through a Haynes #25 sample coated with a complex Mo-Si coating.
4. Evaluation of the hydrogen permeability through tungsten.
5. Evaluation of the permeability of hydrogen through titanium coated Haynes #25.
6. Evaluation of hydrogen permeability of vandium coated 304 Stainless Steel.

Figure 10 indicates the permeability of hydrogen through the Croloy 9M material. The data indicate that at a temperature of approximately 1500°F, a discontinuity in the permeability occurs which corresponds to the $\alpha \longrightarrow \gamma$ transformation. Because of this transformation, the hydrogen permeability through Croloy 9M is greater at 1400°F when it is a body-centered cubic structure than at 1600°F when it a face-centered cubic. The permeability of hydrogen through the Croloy 9M sample at temperatures above the

TABLE I

CSU TEST PARAMETERS

	Endurance			Performance	
	Max.	Mean	Min.	Max.	Min.
Alternator Brg. Supply (T)	410	405	400	450	350
Alternator Brg. Supply (P)	342*	340*	338*	465	280
Thrust Brg. Supply (F)	12.1	11.9	11.8	15.0	8.0
Thrust Brg. Supply (T)	410	405	400	450	350
Thrust Brg. Supply (P)	105	102	100	150	95
Turbine Brg. Supply (F)	6.5	6.4	6.3	8.0	4.4
Turbine Brg. Supply (T)	410	405	400	450	350
Turbine Brg. Supply (P)	385	381	377	440	250
Alternator Brg. (F)	6.5	6.4	6.3	9.8	4.5
Alternator & Thrust Brg. Drain (T)	455	450	445	460	430
Alternator & Thrust Brg. Drain (P)	6.0*	4.2*	3.0*	13.0	1.0
Turbine Brg. Drain (T)	600	595	590	640	380
Turbine Brg. Drain (P)	6.0	5.8	5.5	13.0	5.0
Turbine Inlet (T)	1,265	1,255	1,245	1,270	1,160
Turbine Inlet (P)	242	240	238	265	140
Turbine Exhaust (T)	609	605	601	650	580
Turbine Exhaust (P)	7.5	7.0	6.7	11.5	4.4
Alternator Coolant (T)	552	550	548	579	452
Accelerometer "g" Level	.4	.3	.2	3.0	.2
Hg Pump Discharge (P)	560	495	475	600	415
Hg Pump Discharge (F)	36.0	30	19.5	43.0	0
Hg Pump Inlet (P)	5.5	5.1	4.9	8.0	3.4
Alternator Power	2,850	2,780	2,700	3,760	800
Speed	40,060	40,030	40,000	40,200	0
Acceleration 1/2 Shaft Speed	.2	.05	0	1.2	0
Brg. Clearances - Journals				.00145	.0009
Brg. Clearances - Thrust				.0011	.00085

*Nominal point of 6.4 ppm - Pressure level dependent upon 1/2 speed whirl and flow conditions.
(T) - Temperature °F
(P) - Pressure psig
(F) - Flow lb/min

PERMEABILITY OF HYDROGEN THROUGH CROLOY 9M ALLOY

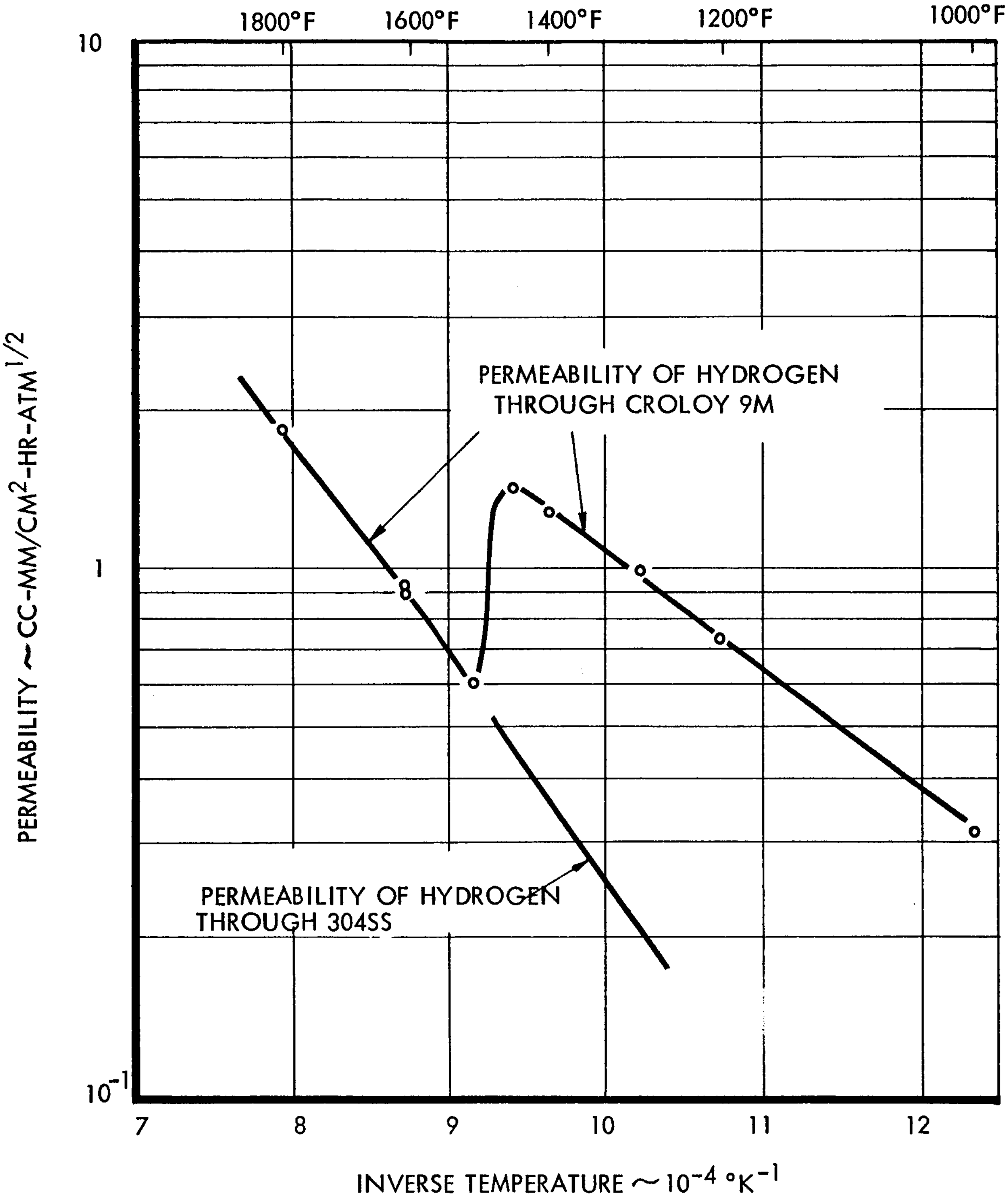

FIGURE 10

transformation is identical to that obtained for 304 stainless steel. The 304 permeability reference is included in the figure.

Figure 11 shows the permeability of the solaramic coated Croloy 9M material. As can be seen from the test, the coating did not afford a barrier to hydrogen and post test examinations have indicated that the solaramic coating did not adhere to the capsule during the test. The difficulty is maintaining the solaramic coating on the material is probably due to the volume change associated with the phase transformation of the material. This results in the general spalling and flaking of the coating, leaving an essentially ineffective barrier.

The Mo-Si coating on the Haynes 25 sample was more inferior as a barrier to hydrogen permeability than either of the previously reported aluminized or W-Si coatings. The data on this capsule are reported in Figure 12.

Evaluations of the permeability of hydrogen through a tungsten sample has shown an anomalous behavior and additional studies are being performed on this coating to determine the experimental difficulties which were encountered. Preliminary subsequent tests of the same material have shown that the tungsten coating exhibits a permeability to hydrogen of approximately 2.0×10^{-3} (cc/hr-cm^2/mm/atm 1/2) at 1600°F. This is represented in Figure 13. The permeability value is exceptionally low and represents a value nearly two orders of magnitude below that of molybdenum. As a result, it represents a good barrier to restrict hydrogen flow.

Figures 14 and 15 show test results which were conducted on titanium coated Haynes #25 and vanadium coated 304 stainless steel. The results show that neither coating provided an effective hydrogen barrier.

Lithium hydride capsule testing was continued throughout the quarter. All static temperature tests at 1600°F have been completed and are presently being sectioned.

Samples are being removed for chemical and metallurgical analysis. A re-evaluation of the program has indicated that a capsule test will be operated with the test objective of one year operation. To date, the capsule has completed 2680 hours of its projected one year life without incident and will be continued toward this objective.

Materials

The workhorse loop has operated throughout the reporting period and evaluations of hydrogen removal and hydrogen swallowing capabilities of the centrifugal pump have been conducted. Hydrogen was injected into the pump through both the superheater and subcooler inlet ports and was removed through a section of Haynes #25 tubing in the condenser section. A columbium window section was also in the condenser. The injection rate, total quantity of hydrogen injected, and the amount of hydrogen removed on the collection port and inlet port are shown in Table II. The temperature of the test rig tubing at the hydrogen collection window in the condenser varied between 600 and 660°F.

PERMEABILITY OF HYDROGEN THROUGH SOLARAMIC COATED CROLOY 9M

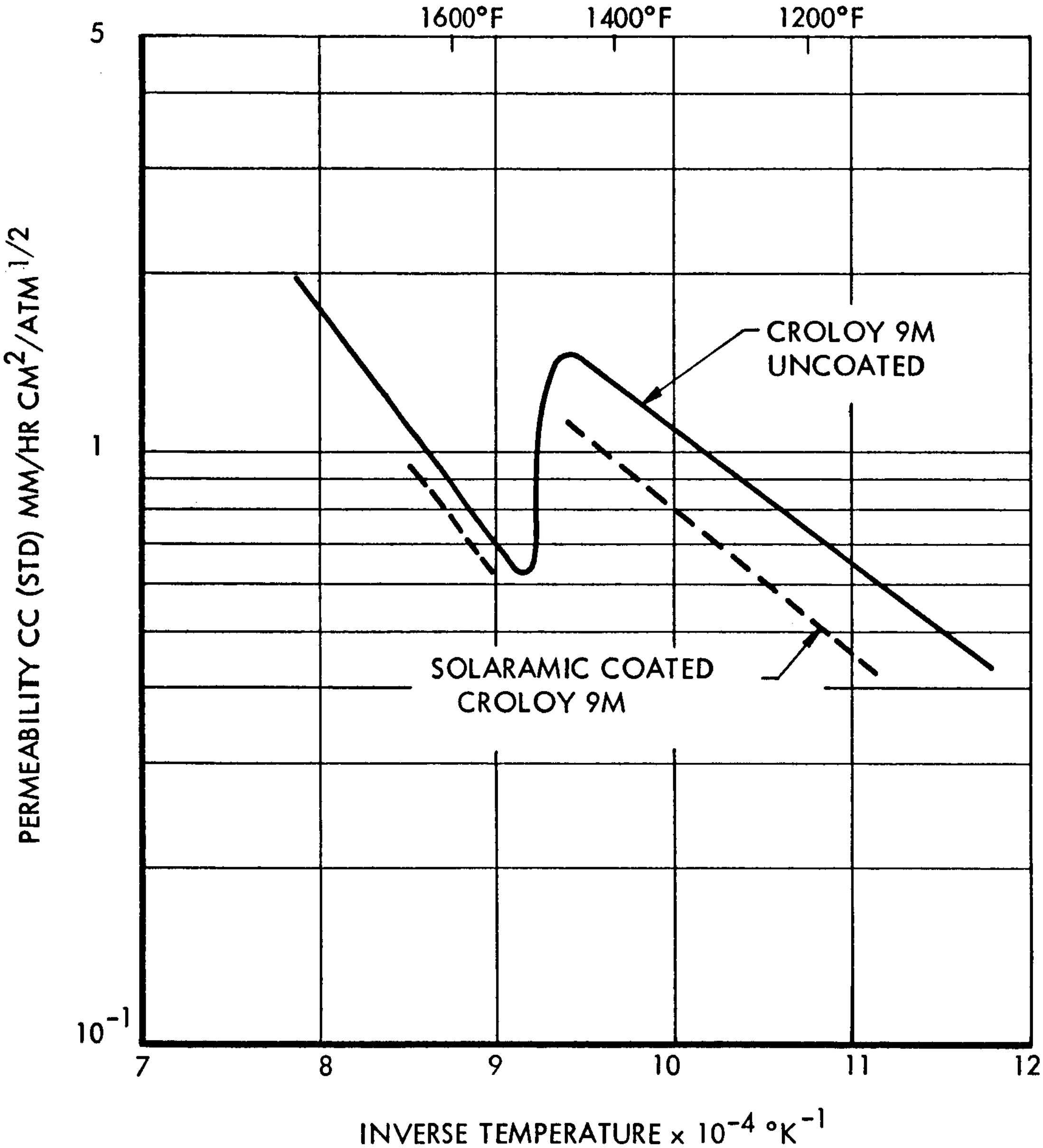

FIGURE 11

PERMEABILITY OF HYDROGEN THROUGH Mo-Si COATING ON HAYNES 25

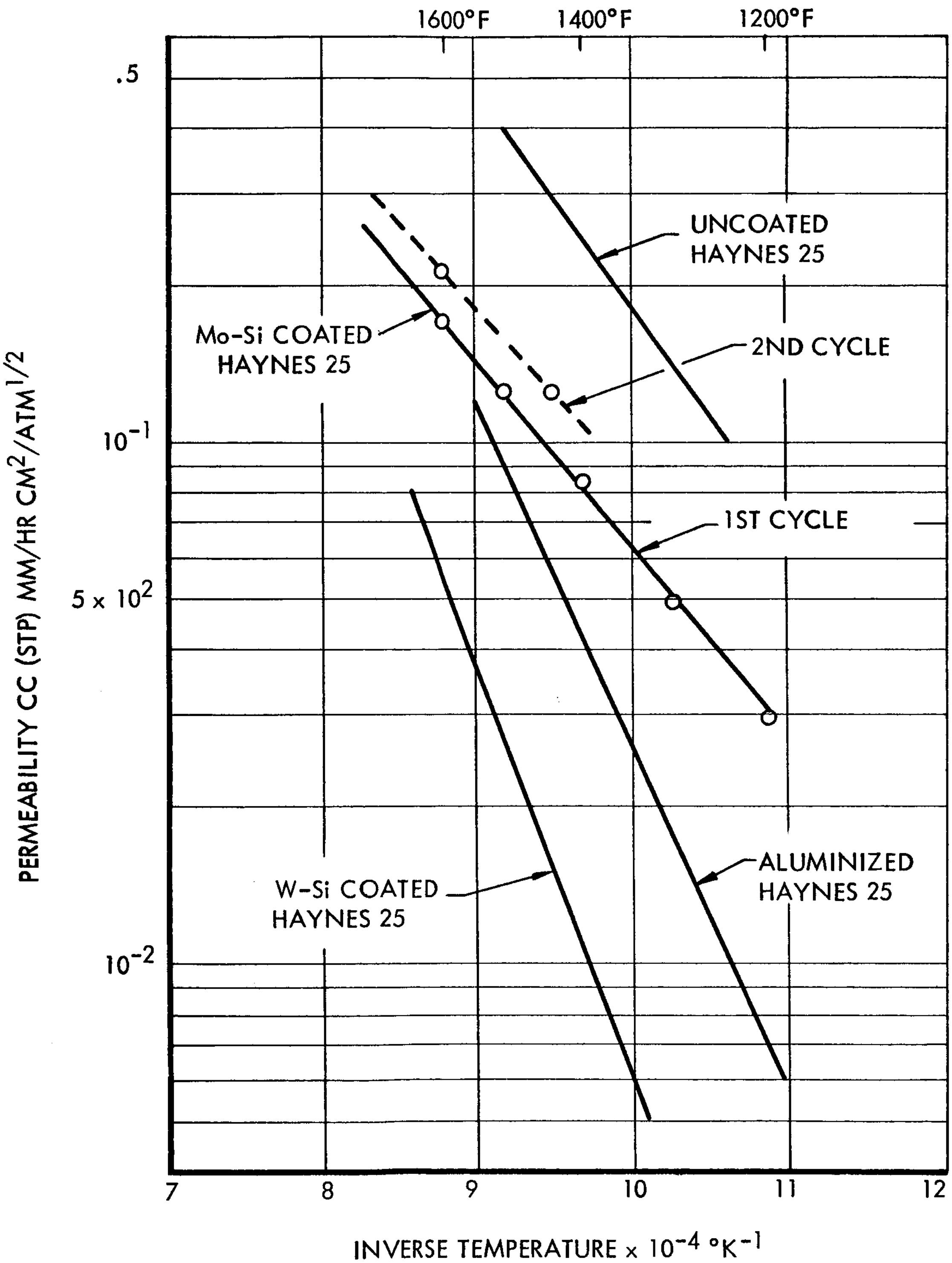

FIGURE 12

PERMEABILITY OF HYDROGEN THROUGH TUNGSTEN (TENTATIVE DATA)

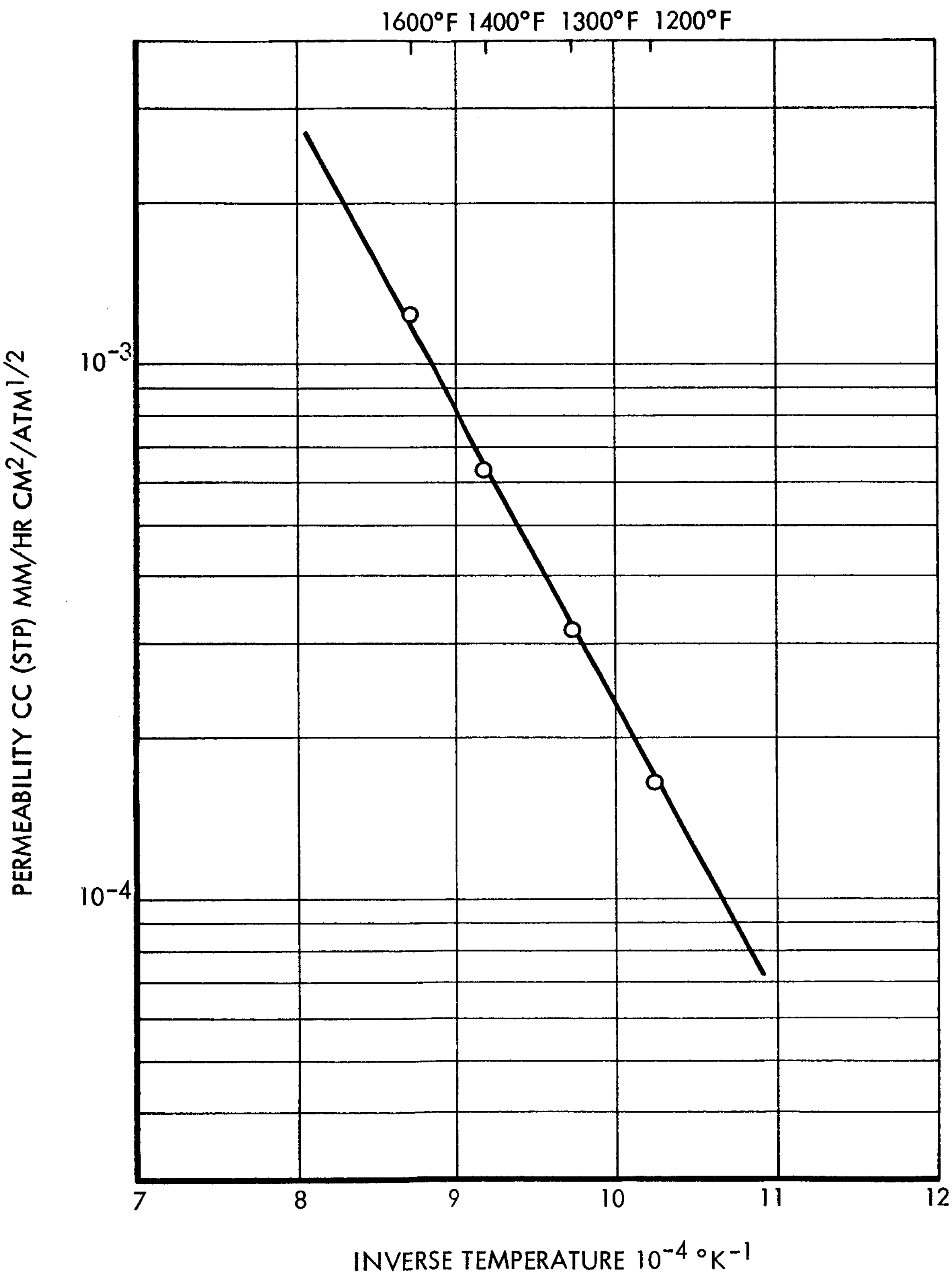

FIGURE 13

PERMEABILITY OF HYDROGEN THROUGH W-SI, TI, VA, AND UNCOATED HAYNES 25

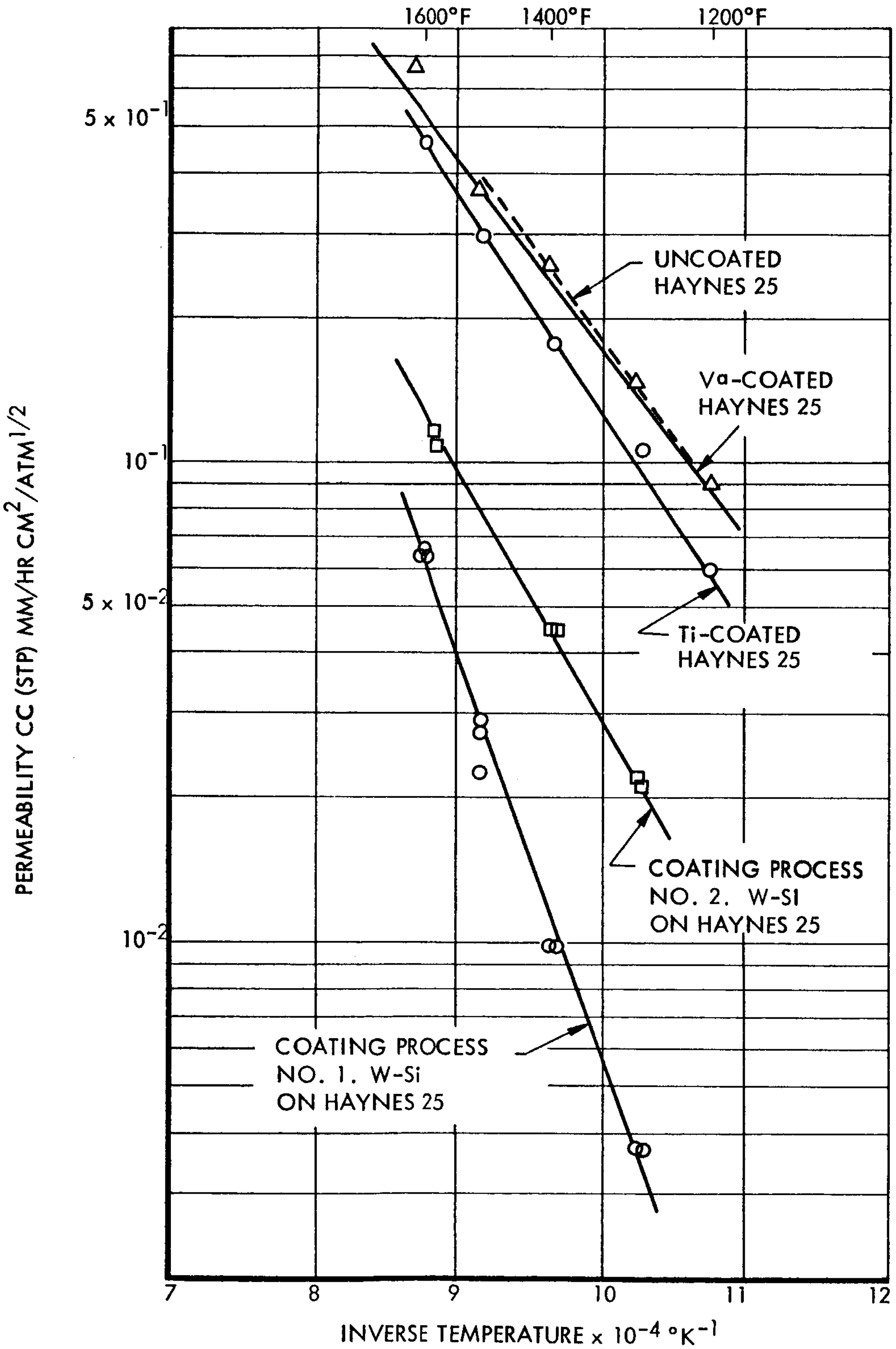

FIGURE 14

PERMEABILITY OF HYDROGEN THROUGH VANADIUM COATED 304SS

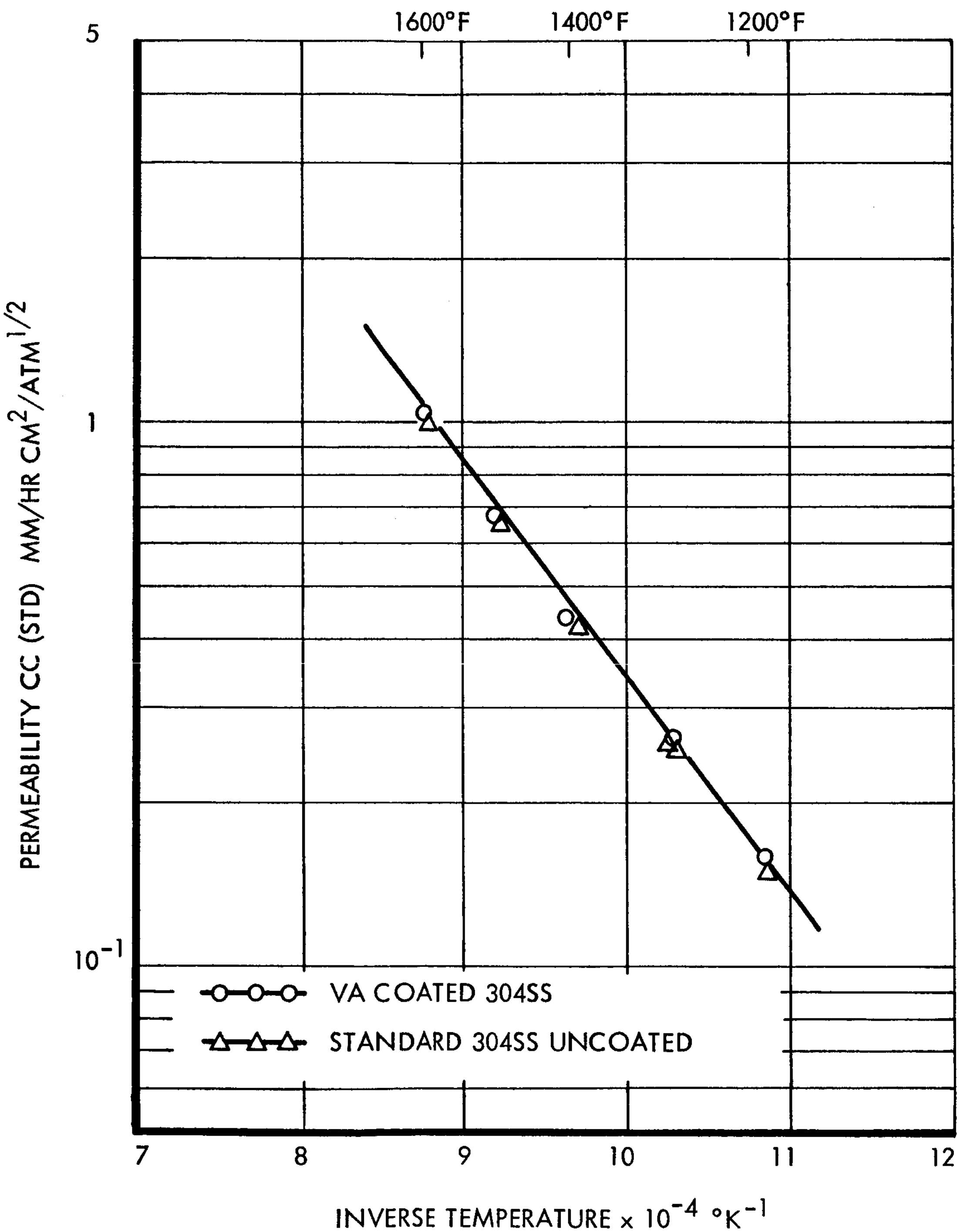

FIGURE 15

TABLE II

SUMMARY OF HYDROGEN REMOVAL RATES FROM THE WORKHORSE LOOP

Injection Rate cc's per Hour	Time & Hours	Total Injected cc's	Collecting Time Hours	Total Collected Hours	Inlet Port	Collecting Points
			Haynes 25 Tubing			
6-7	0.83	5	50	0.02	Superheater	Condenser
9	2.5	22.5	26.7	0.04	Subcooler	Condenser
30	3.0	90	160.7	0.07	Subcooler	Condenser
			Columbium Window			
10	5.5	55	24	0.12	Subcooler	Condenser
7.5	2.67	20	56	Negligible - similar to rig blanking rate	Subcooler	Condenser
14	2.5	35	31.3	"	Superheater	Condenser
74	3.5	259	4.5	"	Superheater	Condenser

The test results indicate that the hydrogen is collecting in the superheater section and is not being transported to the columbium window section where it should diffuse into the collection chambers. The combination of low mercury flow rate and gravity effects are probably trapping the hydrogen in the superheat region of the loop. Without transport of the hydrogen to the window section, the results have been very low. With injection of mercury at other loop stations during the testing, certain loop operating conditions of flow resulted in transient hydrogen transport to the columbium window section. In such instances, the diffusion of hydrogen through the window occurred at significant rates. Because it was a erratic operation, no actual test data were obtained other than visual observation of the pressure rise in the collection chamber. It does indicate, however, that if the problems of transporting hydrogen to the window can be solved, the window technique may be quite acceptable.

The second test being conducted with the activities on the workhorse loop includes evaluation of the hydrogen swallowing capabilities of the mercury centrifugal pump. The pump was replaced in the loop after repair of the rubber "O" ring seals and several tests were conducted to determine its operating conditions. Dead head tests were conducted with both a 30 inch head and a 8.5 psia inlet pressure to determine the maximum output pressure. In both conditions, the pump delivered 600 psia discharge pressure at relatively high rotating speeds. Additional checks were made to determine the threshold pressure at which leakage occurred at the dynamic seal. The results indicated that the pump will operate at high speeds and high outlet pressures with minimum seal leakage. Additional changes have included replacement of the loop by-pass line with a new manual control valve and associated plumbing. The hardware changes are being made to obtain better by-pass flow control and allow more stable operating conditions to exist in the pump before further evaluations are conducted.

Hydrogen swallowing tests of the centrifugal pump were conducted by injecting a known volume of hydrogen gas into the inlet of the centrifugal pump. The volume of succeeding gas bubbles was then increased, with the pump operating at steady state conditions until loss of prime of the centrifugal pump was noted. The results of the testing are presented in Table III.

These results are encouraging in that the pump appears to exhibit the ability to pass relatively large volumes of hydrogen gas without losing prime. Continued tests will be conducted at various inlet heads to continue evaluations of hydrogen handling capabilities. The next series of tests will be conducted under the same conditions except that the inlet pressure will be raised to 8.5 psia.

The Haynes 25 workhorse loop has accumulated in excess of 3600 hours of operation in the current series of test.

Work on the trapping of mercury corrosion products has progressed throughout the quarter. The corrosion loop was started at the beginning of the reporting period, following a minor repair to the boiler heater. The loop had operated continuously for a period of 693 hours prior to a forced shut down due to a leak in the bellows of a Haynes #25 throttling valve in the superheater. It was operated for this period of time under the following conditions:

TABLE III

CENTRIFUGAL PUMP HYDROGEN SWALLOWING CAPABILITY

Inlet Pressure psia	Outlet Pressure psia	Pump Speed rpm	Critical Bubble Size to Cause Loss of Prime cc*
4	216	30,300	0.6
4	216	32,600	0.6
4	296	31,500	0.4
4	311	32,700	Up to 1.2 cc per bubble, no loss of prime.**
4	361	34,700	Up to 1.4 cc per bubble, no loss of prime.**
5.5	200	37,500	.9 cc
5.5	250	34,500	.7 cc
5.5	300	34-36,000	.8 - 1.0

*Bubble size is at STP prior to being injected into system.

**In these instances, the bubbles above 0.8 cc probably broke up into smaller size bubbles before reaching the pump.

1. Boiler outlet - 1096 - 1100°F

2. Superheater - 1300°F

3. Superheater wall - 1465°F

4. Condenser - 655-670°F

5. Subcooler - 210°F

6. Flow Rate - 68-128 lb/hr

After shut down of the rig for repair of the throttling valve bellows, a small weld crack was noted in a longitude weld in the corrosion product separator of the superheater. This weld imperfection was repaired. During the interim period, new heaters were installed on the corrosion product separator in order to raise the temperature of the liquid in the separator section. Controls for the heater were mounted and wired to the test consoles.

The Haynes #25 valves were returned from the vendor and installed in the loop. During leak checking, the bellows and the hand operated valve were again found defective. In order to reduce the amount of down time with the loop, an orifice was fabricated and installed in series with an air operated valve and nozzle. Thus, manual adjustment of the valve would allow fine control over the throttling process. The loop was restarted and has been operating under the following conditions:

1. Boiler outlet - 1096°F

2. Superheater Wall Temperature - 1400°F

3. Condenser - 688°F

4. Subcooler - 180°F

5. Flow Rate - 40-70 lb/hr

The corrosion loop in the series of tests conducted thus far has operated in excess of 850 hours of operation.

IV. CURRENT PROBLEM AREAS

The only significant problem area which has been encountered during this period is the failure of bellows of two Haynes #25 throttling valves in the corrosion product trapping loop. The malfunction of these two valves has caused the loss of approximately two months of test time. Due to the length of time involved for vendor repair, the loop will be operated with a fixed orifice and nozzle for the remainder of the test time assuming satisfactory loop operating conditions can be obtained with the orifice-nozzle combination.

V. PLANNED DIRECTION OF EFFORT FOR THE NEXT QUARTER

Endurance testing of turbo-alternator CSU I-3A will be continued.

Operation of the workhorse loop will be continued, and shall be directed toward evaluating the hydrogen removal capabilities of a centrifugal separator. In addition, testing of the hydrogen swallowing of the jet centrifugal pump will be continued.

The force circulation mercury corrosion loop testing will be continued on its endurance test objectives.

Work on Solar Collector and Condenser Subcooler Topical Reports will be continued.

System troubles.

Haynes 25 Valves
Lithium Hydrogen Containment
Mercury pump seals.

DISTRIBUTION LIST

	No. of Copies
National Aeronautics & Space Administration 1512 H Street, Northwest Washington 25, D.C. Attention: Walter Scott (RP)	1
National Aeronautics & Space Administration 1512 H Street, Northwest Washington 25, D.C. Attention: Herbert Rochen (RNEP)	1
Ames Research Center National Aeronautics & Space Administration Moffett Field, California Attention: Librarian	1
Goddard Space Flight Center National Aeronautics & Space Administration Washington 25, D.C. Attention: Milton Schach, Code 630, Bldg. NRL-101	1
Langley Research Center National Aeronautics & Space Administration Hampton, Virginia Attention: Emanuel Schnitzer	1
Lewis Research Center National Aeronautics & Space Administration 21000 Brookpark Road Cleveland 35, Ohio Attention: Richard P. Geye, SEPO, OPM	1
Lewis Research Center National Aeronautics & Space Administration 21000 Brookpark Road Cleveland 35, Ohio Attention: Henry O. Slone, SEPO, OPM	1
Lewis Research Center National Aeronautics & Space Administration 21000 Brookpark Road Cleveland 35, Ohio Attention: Librarian	1

DISTRIBUTION LIST (Continued)

	No. of Copies
Marshall Space Flight Center National Aeronautics & Space Administration Huntsville, Alabama Attention: George C. Bucher, Code RPD	1
Marshall Space Flight Center National Aeronautics & Space Administration Huntsville, Alabama Attention: Josef F. Blumrick, Code S & MD	1
AiResearch Manufacturing Division The Garrett Corporation Phoenix, Arizona Attention: William Bowler	1
Allison Division General Motors Corporation Indianapolis 6, Indiana Attention: T. F. Nagey	1
Advanced Research Projects Agency Room 3E 153, The Pentagon Washington 25, D.C. Attention: Dr. Urner Liddell	1
Chance Vought Aircraft, Inc. P.O. Box 5907 Dallas 22, Texas Attention: Thomas Dolan	1
Convair-Astronautics 5001 Kearny Villa Road San Diego 11, California Attention: Krafft A. Ehricke	1
Electro-Optical Systems, Inc. 125 N. Vinedo Avenue Pasadena, California Attention: James H. Fisher	1

DISTRIBUTION LIST (Continued)

	No. of Copies
Air Force Systems Command Aeronautical Systems Division Flight Accessories Laboratory Wright Patterson Air Force Base, Ohio Attention: C. H. Armbruster, ASRMFP	1
Air Force Systems Command Aeronautical Systems Division Flight Accessories Laboratory Wright Patterson Air Force Base, Ohio Attention: Donald Mortel	1
General Electric Company Missile & Space Vehicle Department 3198 Chestnut Street Philadelphia 4, Pennsylvania Attention: Edward Ray	1
Institute for Defense Analysis Universal Building 1825 Connecticut Avenue, N.W. Washington 9, D.C. Attention: Robert Hamilton	1
Jet Propulsion Laboratory California Institute of Technology Pasadena, California Attention: Garth E. Sweetnam	1
Jet Propulsion Laboratory California Institute of Technology Pasadena, California Attention: Librarian	1
Lockheed Missile & Space Division Sunnyvale, California Attention: Charles Burrell	1
Pratt & Whitney Aircraft 400 Main Street East Hartford 8, Connecticut Attention: William Podolny	1

DISTRIBUTION LIST (Continued)

	No. of Copies
Space Technology Laboratories P.O. Box 95001 Los Angeles 45, California Attention: George E. Mueller	1
Sundstrand Denver 2480 W. 70th Avenue Denver 21, Colorado Attention: Robert Boyer	1
Air Force Systems Command Ballistic Systems Division Inglewood, California Attention: WDAT-60-886-6/Mrs. Sangonard/3039	1
U.S. Army Signal Research Development Laboratory Fort Monmouth, New Jersey Attention: Arthur Daniel	1
Aerojet General Corporation Azusa, California Attention: Paul I. Wood	1
Atomics International P.O. Box 309 Canoga Park, California Attention: Chief Librarian, 61-AT 2612	1
Boeing Airplane Company Aero-Space Division Seattle 24, Washington Attention: John S. Miller, 2-5454, Mail Stop 19-12	1
Atomics International P.O. Box 309 Canoga Park, California Attention: Joseph Wetch	1
Project Analysis Section General Electric Research Lab. P.O. Box 1088 Schenectady, New York Attention: V. C. Wilson	1

DISTRIBUTION LIST (Continued)

	No. of Copies
Project Analysis Section General Electric Research Lab. P.O. Box 1088 Schenectady, New York Attention: W. Adair Morrison	1
Lewis Research Center National Aeronautics & Space Administration 21000 Brookpark Road Cleveland 35, Ohio Attention: Bernard Lubarsky	1
Director, USAF Project RAND Via, Air Force Liaison Office The Rand Corporation 1700 Main Street Santa Monica, California Attention: Library	1
Air Force Systems Command Aeronautical Systems Division Wright-Patterson Air Force Base, Ohio Attention: B. Chasman (ASRCE)	1
Joel Levy, Manager United States Atomic Energy Commission Canoga Park Area Office P.O. Box 591 Canoga Park, California	1
Westinghouse Electric Corporation P.O. Box 989 Lima, Ohio Attention: D. F. Rife Advanced Systems Application Dept.	1
Lewis Research Center Space Electric Power Procurement Office 21000 Brookpark Road Cleveland 35, Ohio Attention: John J. Fackler	1

DISTRIBUTION LIST (Continued)

	No. of Copies
Lewis Research Center 21000 Brookpark Road Cleveland 35, Ohio Attention: N. T. Musial Patent Counsel	1
Air Force Systems Command Aeronautical Systems Division Wright Patterson Air Force Base, Ohio Attention: Robert A. Green (ASNPFS)	1
Lewis Research Center National Aeronautics & Space Administration 21000 Brookpark Road Cleveland 35, Ohio Attention: J. A. Heller, APGO 86-1	2
Lewis Research Center National Aeronautics & Space Administration 21000 Brookpark Road Cleveland 35, Ohio Attention: R. L. Cummings, APGO 86-1	1
National Aeronautics & Space Administration Scientific and Technical Information Facility Box 5700 Bethesda 14, Maryland Attention: NASA Representative	2 plus reproducible
National Aeronautics & Space Administration 1512 H Street, Northwest Washington 25, D. C. Attention: John Sloop (RP)	1
Mr. Bernard M. Lehv Orgn. 2-5724 Mail Stop 22-68 The Boeing Company Aero-Space Division Seattle, Washington	1

CROLOY 9M

SOLARAMIC COATED CROLOY 9M.

HAYNES #25 COATED WITH MO-SI COATING.

TUNGSTEN

TITANIUM COATED HAYNES #25

VANAD COATED 304 STAINLESS STEEL.

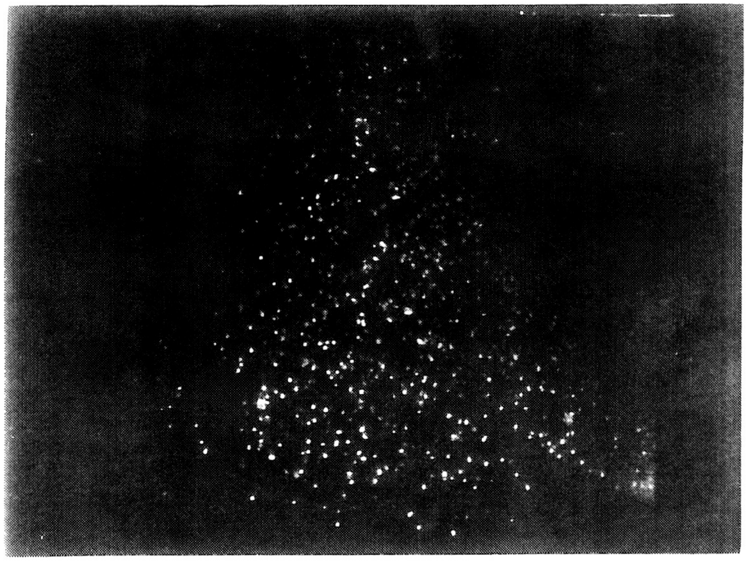

Fig. 1, Canis Minor, 2 sec., 2:30 A.M.

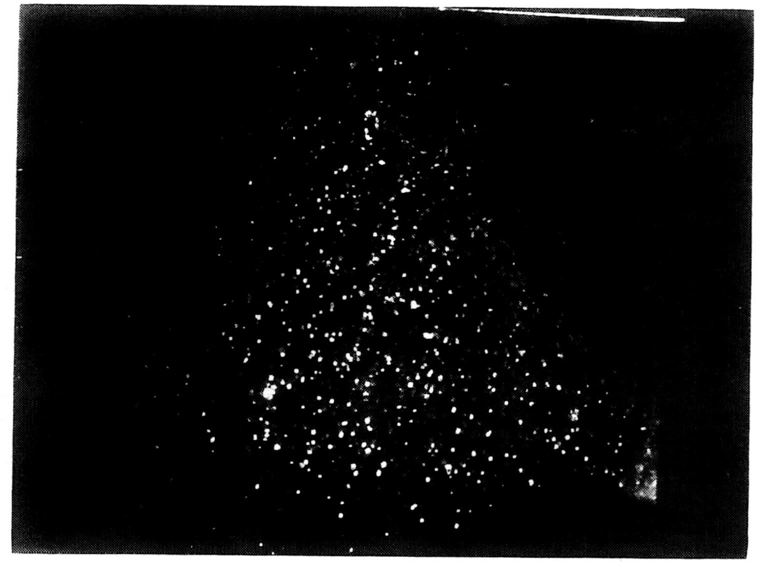

Fig. 2, Canis Minor, 2 sec., 2:35 A.M.

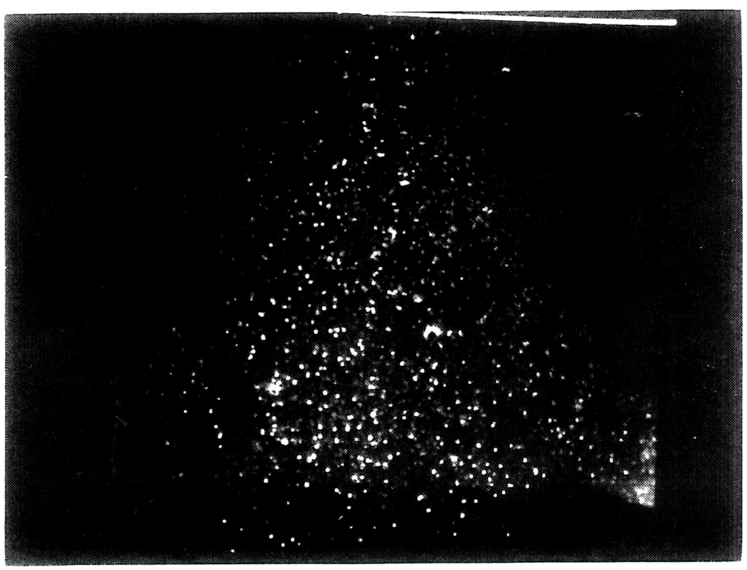

Fig. 3, Canis Minor, 2 Sec., 2:40 A.M.

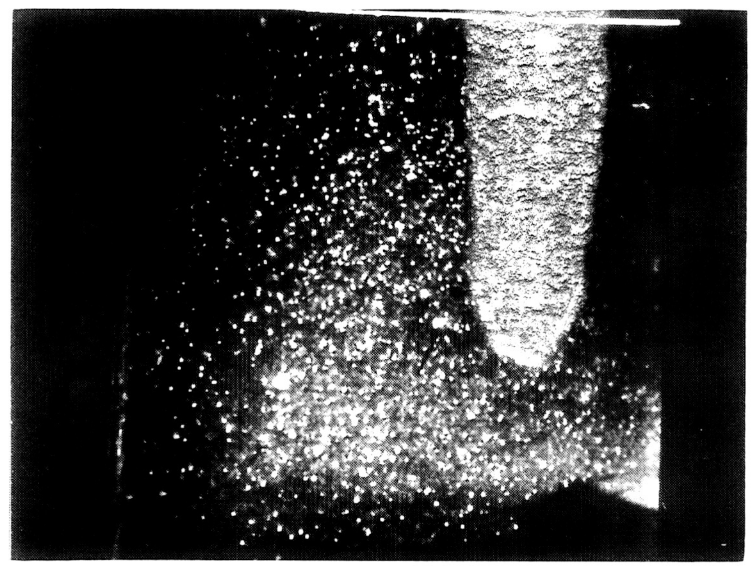

Fig. 4, Canis Minor, 2 Sec., 2:45 A.M.

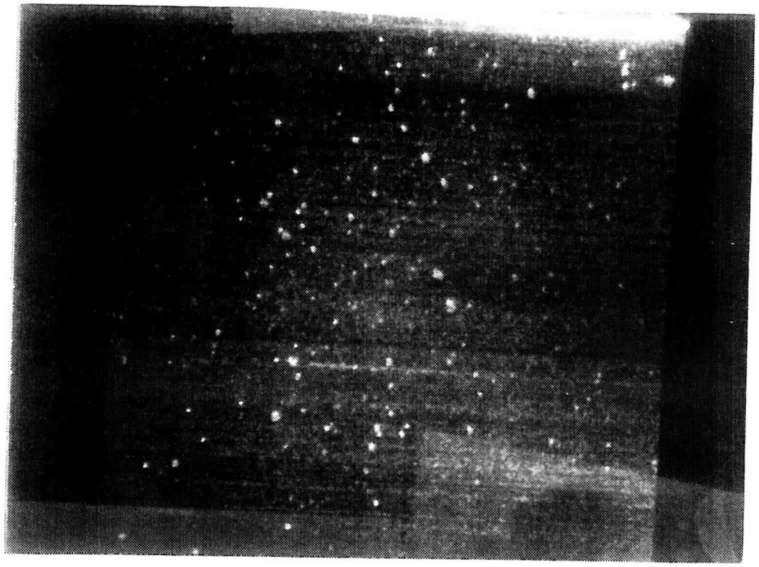

Fig. 5, Canis Minor, 2 Sec., 0.8 ND filter, 3:00 A.M.

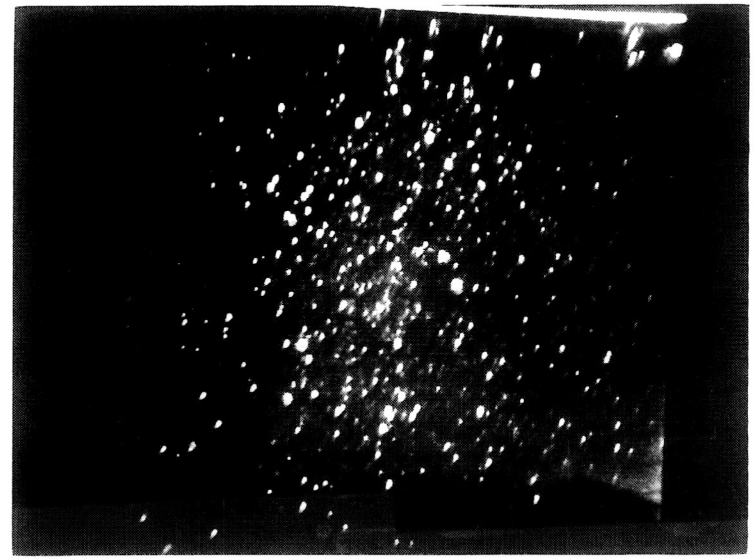

Fig. 6, Canis Minor, 8 Sec., 0.8 ND filter, 3:10 A.M.

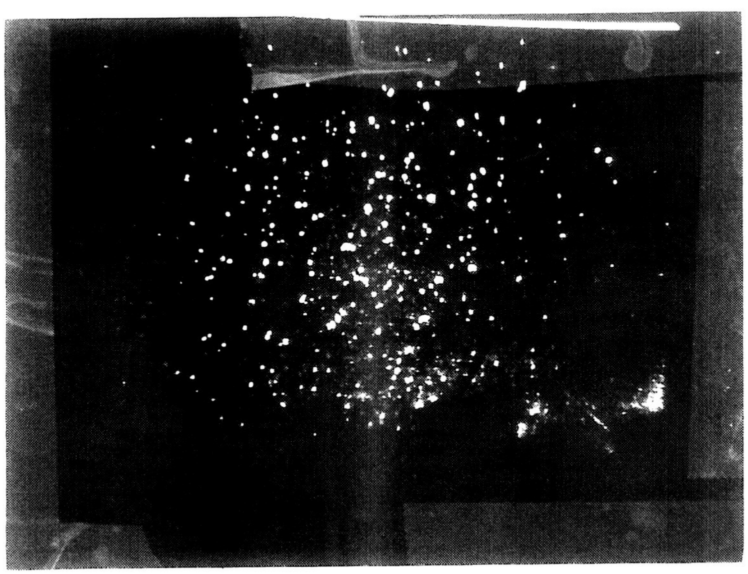

Fig. 7, Ursa Major, 8 Sec., 0.8 ND filter, 4:50 A.M.

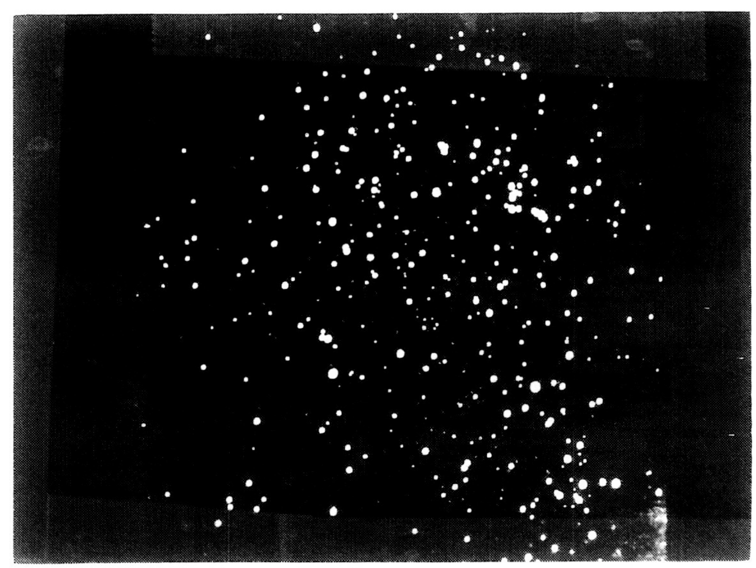

Fig. 8, Canis Minor, Orion, 2 Sec., 92.0 V, 2:55 A.M.

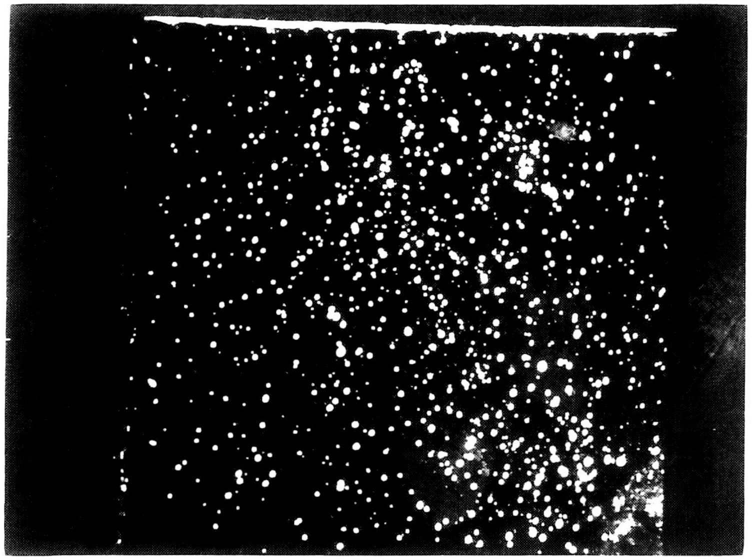

Fig. 13, Canis Minor, Orion, 16 Sec.,
92.0 V. 3:06 A.M.

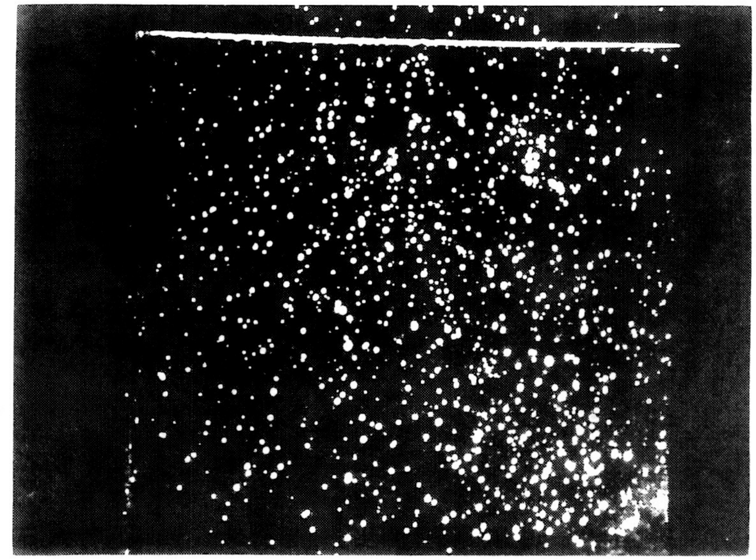

Fig. 14, Canis Minor, Orion, 32 Sec.,
92.0 V, 3:07 A.M.

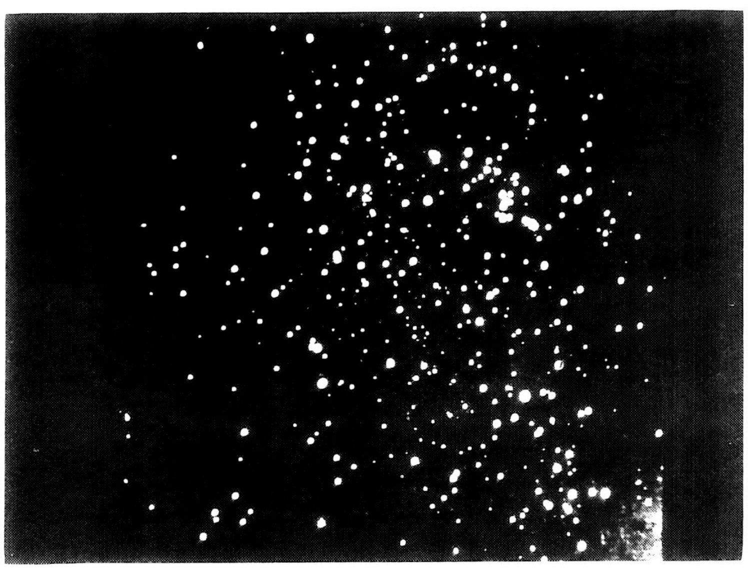

Fig. 15, Canis Minor, Orion, 2 Sec.,
92.0 V, 3:10 A.M.

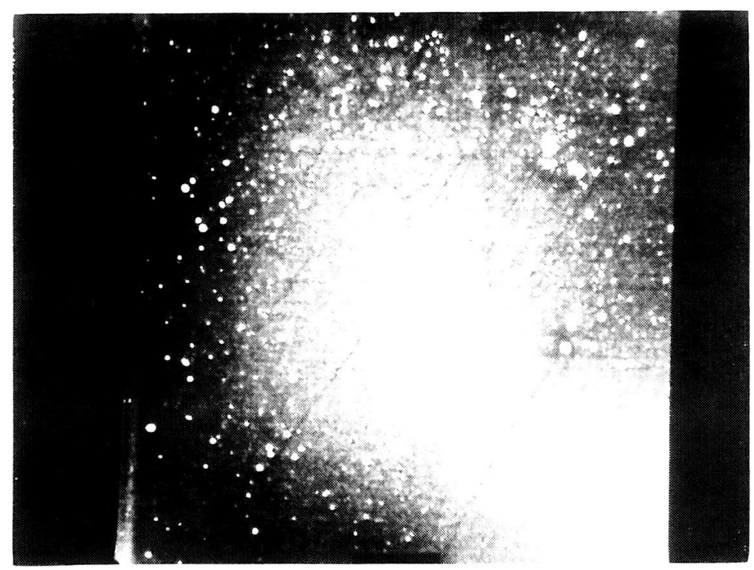

Fig. 16, Canis Minor, Orion, 2 Sec.,
92.0 V, 3:15 A.M.

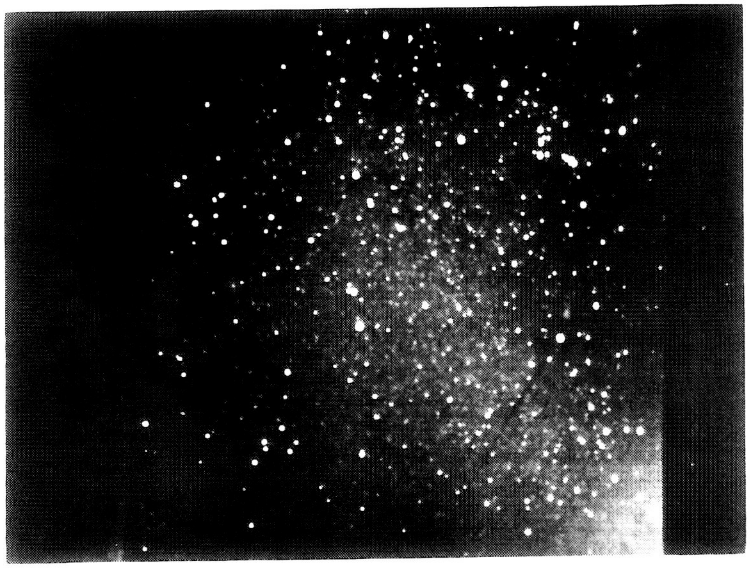

Fig. 17, Canis Minor, Orion, 2 Sec., 92.0 V, 3:20 A.M.

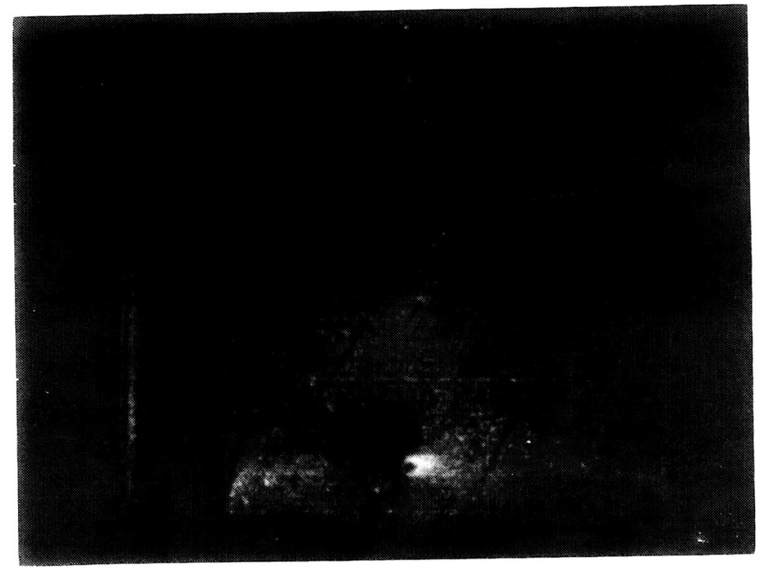

Fig. 18, Leo, Venus, Zodiacal Light, 2 Sec., 93.0 V, 3:35 A.M.

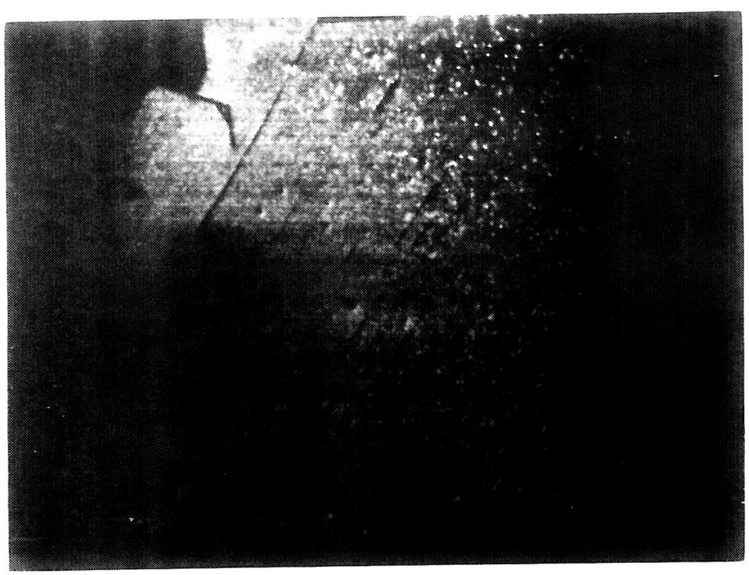

Fig. 19, Leo, Venus, Zodiacal Light, 2 Sec., 93.0 V, 3:50 A.M.

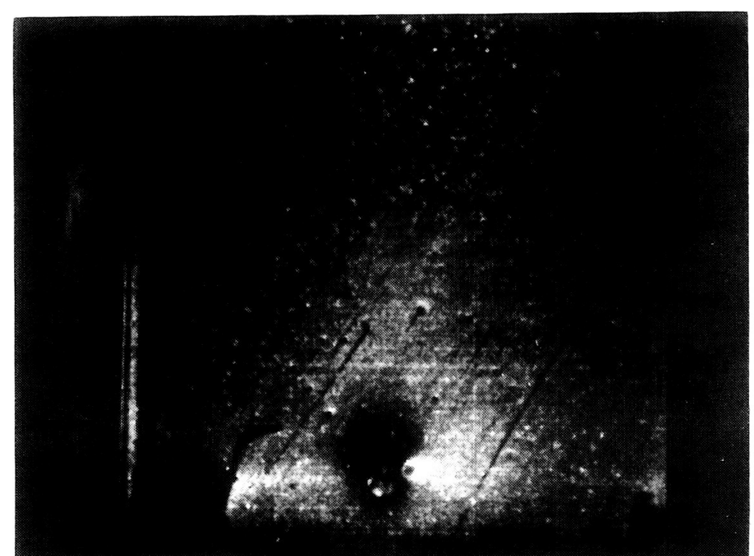

Fig. 20, Leo, Venus, Zodiacal Light, 2 Sec., 93.0 V, 3:53 A.M.

Fig. 21, Leo, Venus, Zodiacal Light, 2 Sec.,
93.0 V, 3:59 A.M.

Fig. 22, Leo, Venus, Zodiacal Light, 2 Sec.,
93.0 V, 4:00 A.M.

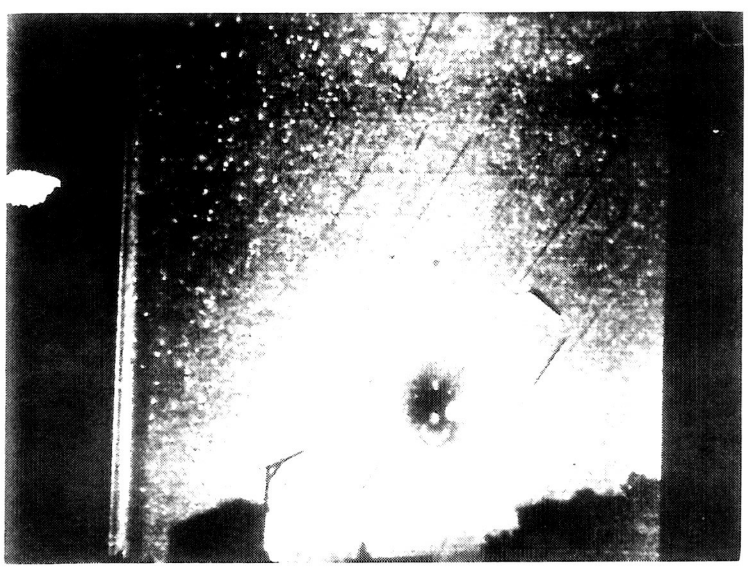

Fig. 23, Leo, Venus, Zodiacal Light, 2 Sec.,
93.0 V, 4:05 A.M.

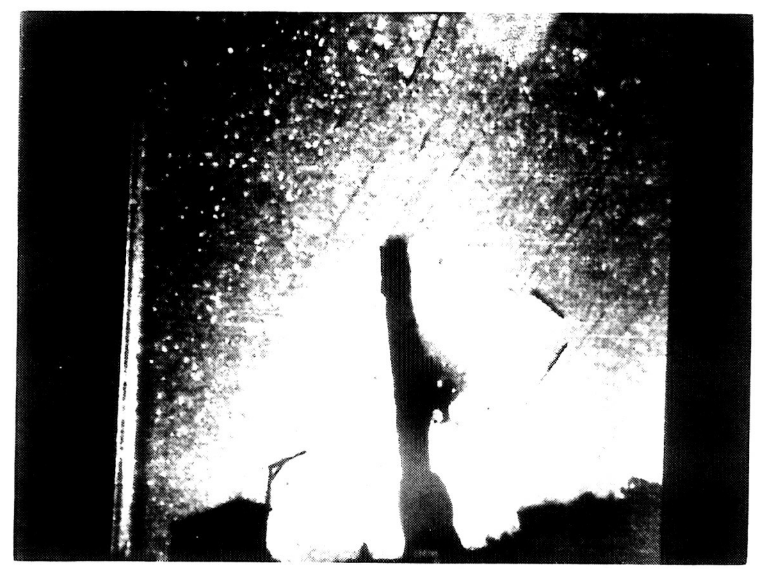

Fig. 24, Leo, Venus, Zodiacal Light, 2 Sec.,
93.0 V, 4:07 A.M.

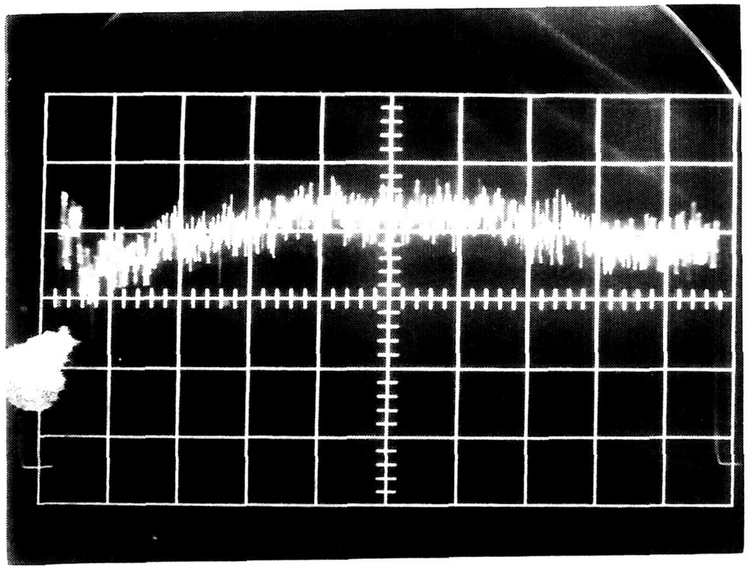

Fig. 25, Oscillogram of single trace just above middle of Fig. 23.

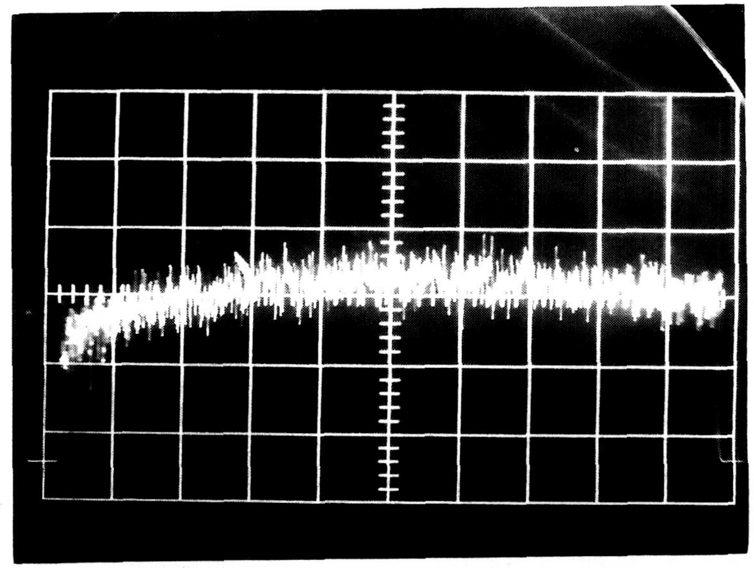

Fig. 26, Oscillogram of same trace as in Fig. 25 but with lens capped.

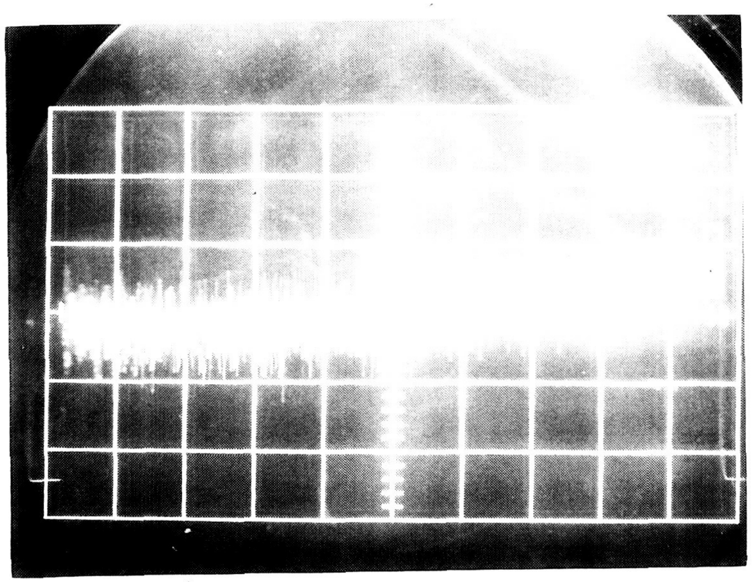

Fig. 27, Oscillogram of trace near bottom of frame with lens capped.

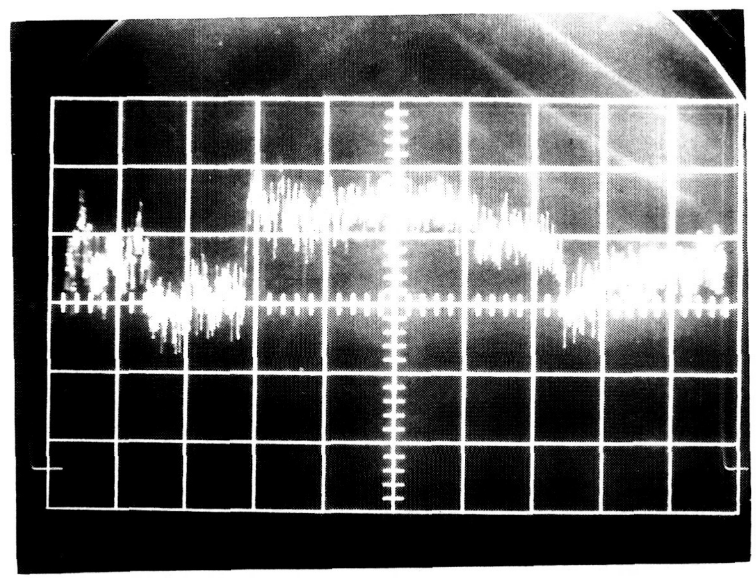

Fig. 28, Oscillogram of same trace as in Fig. 27 but with lens open to field of Fig. 23.

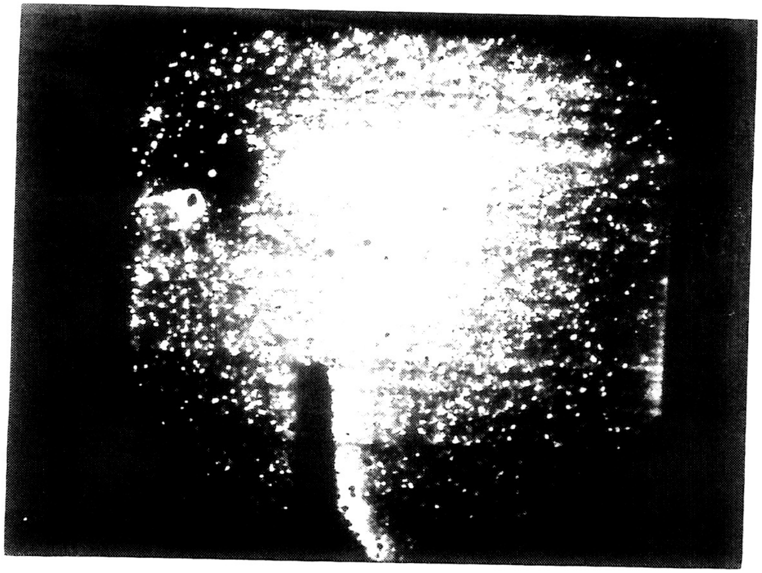

Fig. 29, Eridanus, Taurus, Jupiter, 2 Sec.,
92.9 V, 12:55 A.M.

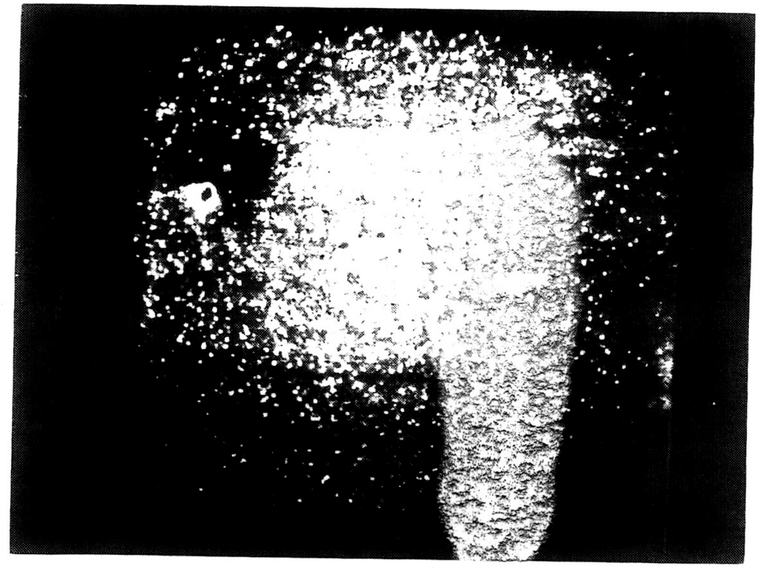

Fig. 30, Eridanus, Taurus, Jupiter, 2 Sec.,
92.9 V, 12:5[illegible] A.M.

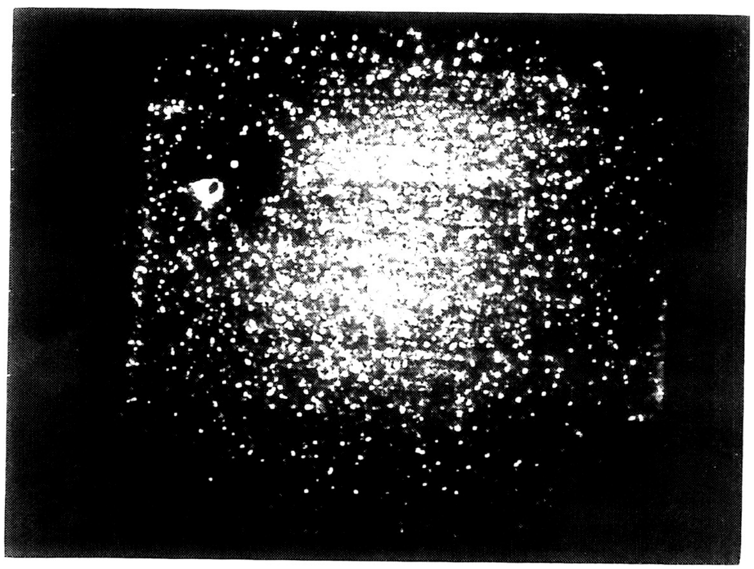

Fig. 31, Eridanus, Taurus, Jupiter, 2 Sec.,
92.8 V, 1:00 A.M.

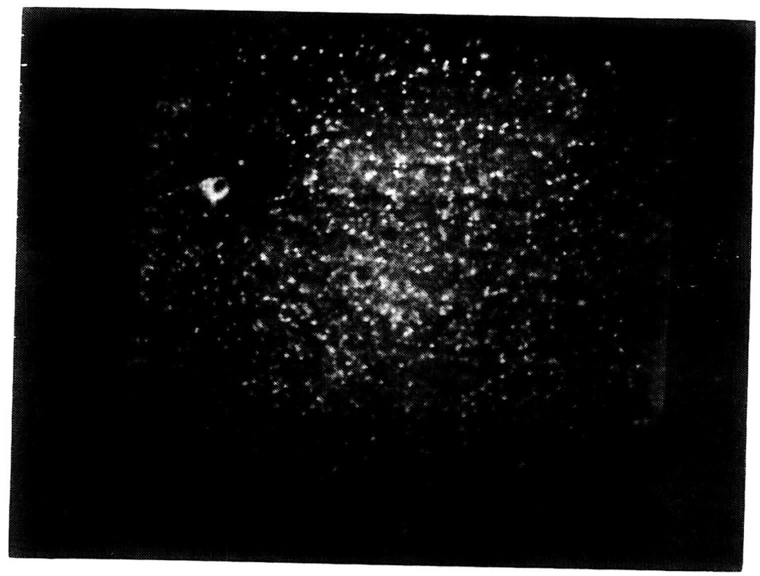

Fig. 32, Eridanus, Taurus, Jupiter, 2 Sec.,
92.8 V, 1:05 A.M.

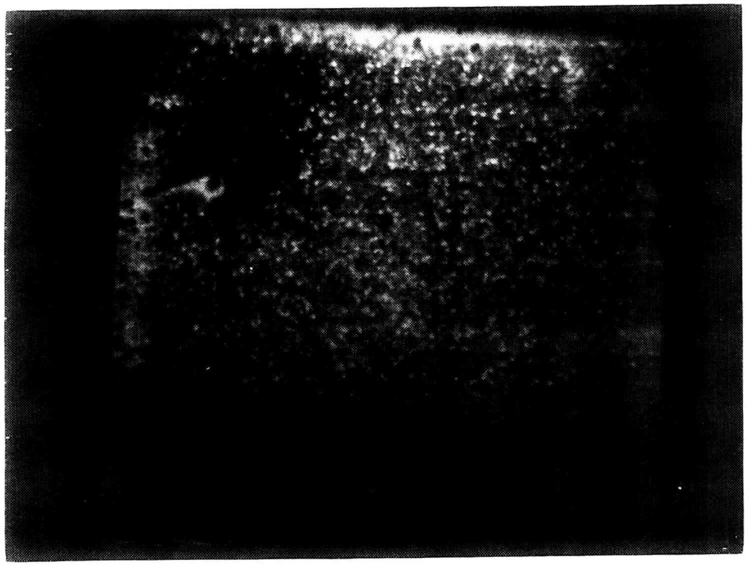

Fig. 33, Eridanus, Taurus, Jupiter, 4 Sec.,
92.8 V, 1:06 A.M.

Fig. 34, Eridanus, Taurus, Jupiter, 2 Sec.,
92.8 V, 1:15 A.M.

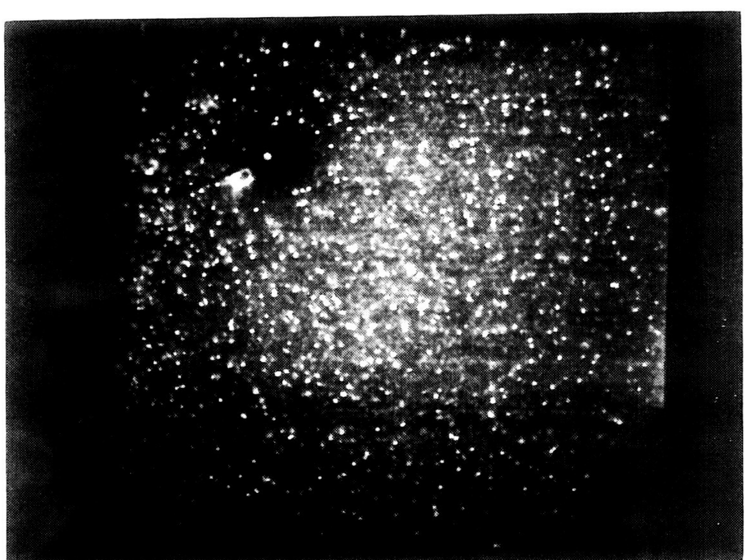

Fig. 35, Eridanus, Taurus, Jupiter, 2 Sec.,
92.6 V, 1:20 A.M.

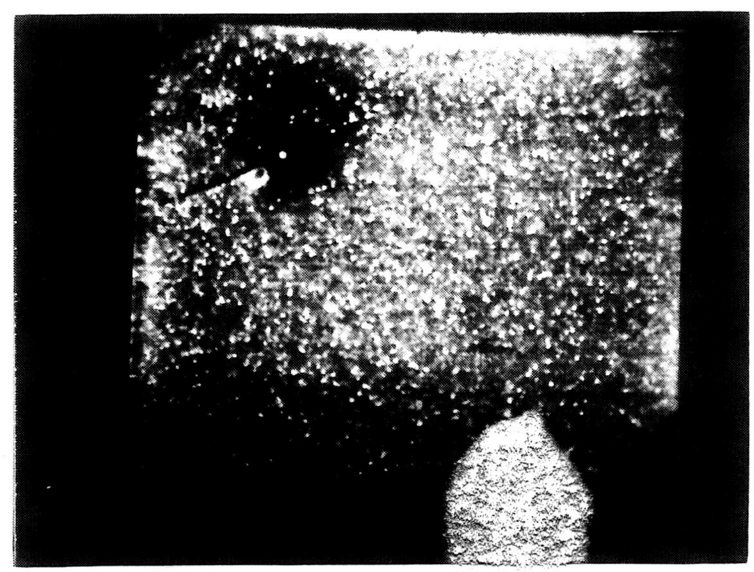

Fig. 36, Eridanus, Taurus, Jupiter, 4 Sec.,
92.6 V, 1:22 A.M.

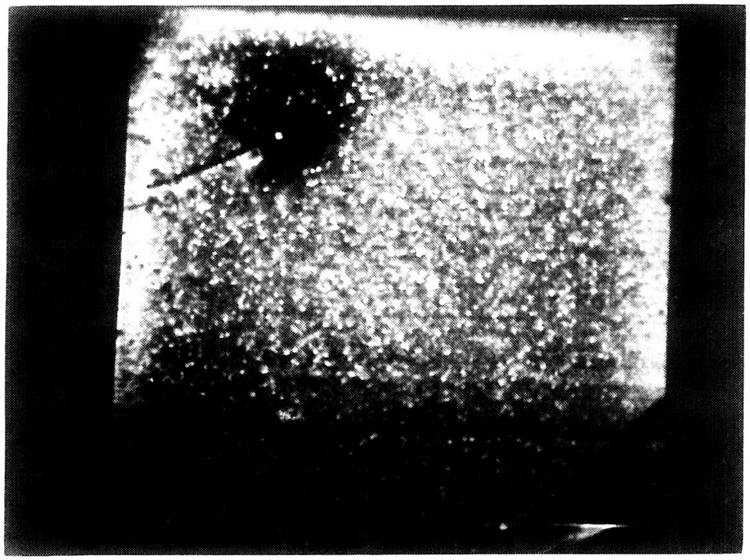

Fig. 37, Eridanus, Taurus, Jupiter, 8 Sec., 92.6 V, 1:25 A.M.

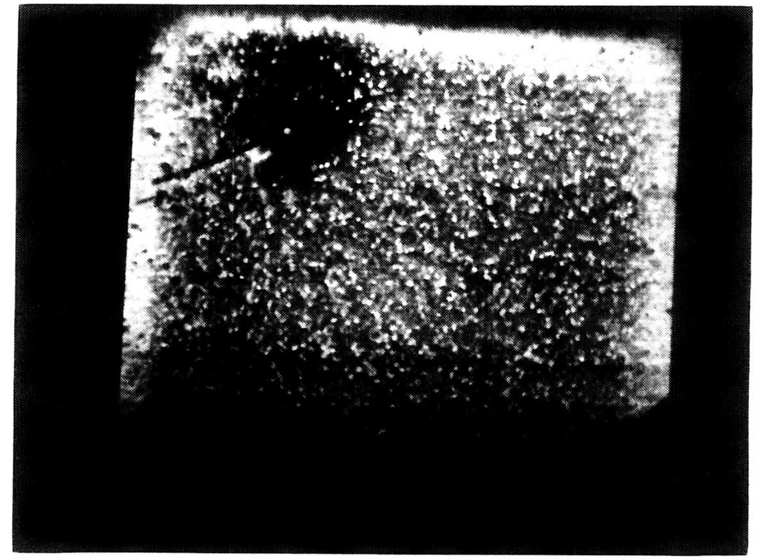

Fig. 38, Eridanus, Taurus, Jupiter, 16 Sec., 92.6 V, 1:27 A.M.

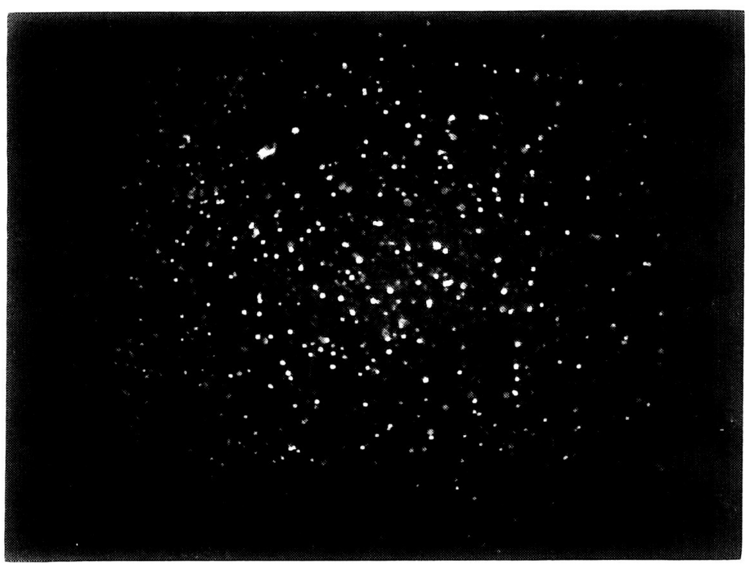

Fig. 39, Eridanus, Taurus, Jupiter, 2 Sec., 92.3 V, 1:35 A.M.

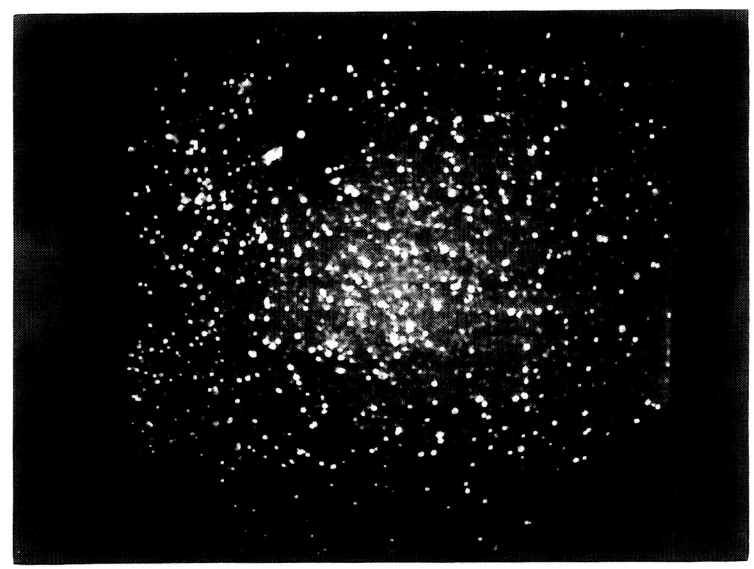

Fig. 40, Eridanus, Taurus, Jupiter, 2 Sec., 92.3 V, 1:36 A.M.

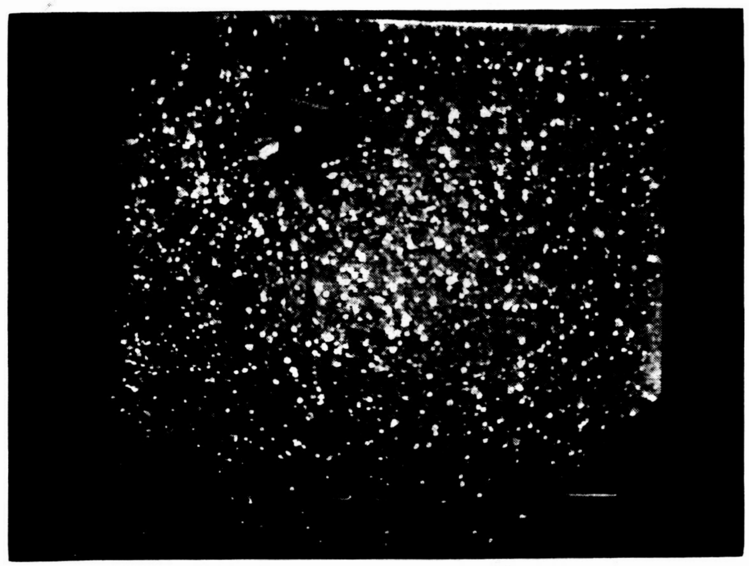

Fig. 41, Eridanus, Taurus, Jupiter, 4 Sec., 92.3 V, 1:40 A.M.

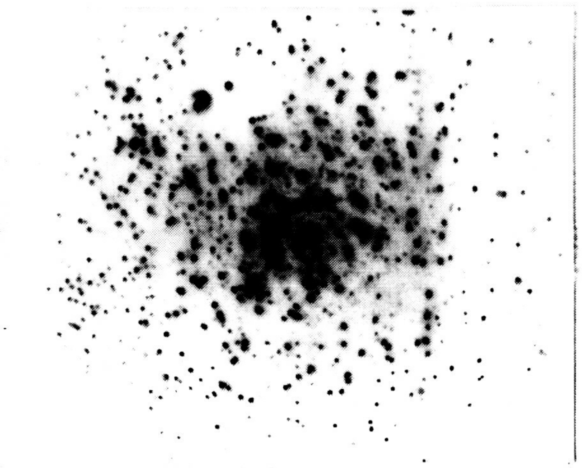

Fig. 42, Jupiter, Taurus, Eridanus, 2 sec., 92.3V, 2:00 A. M.

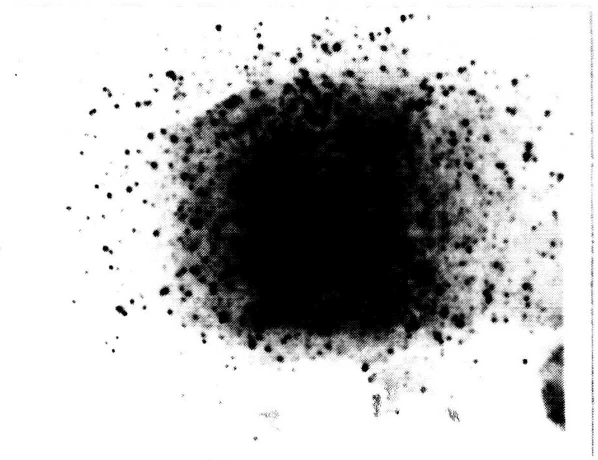

Fig. 43, Ursa Major, 2 sec., 92.3V 2:05 A. M.

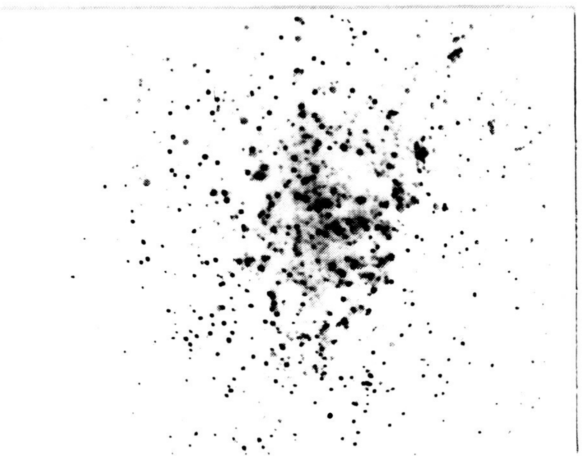

Fig. 44, Andromeda, Cassiopeia, 2 sec., 92.3V, 2:15 A. M.

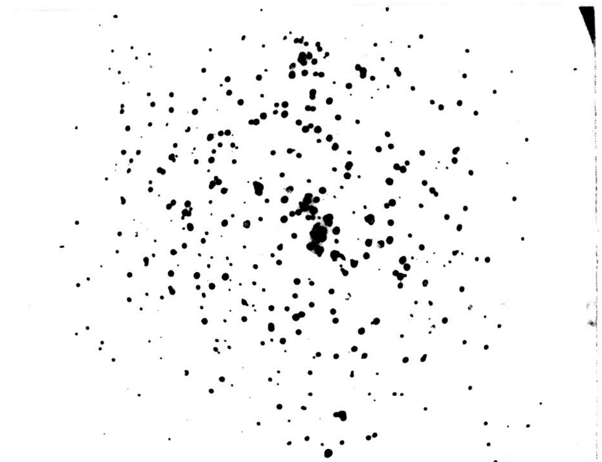

Fig. 45, Orion, 2 sec., 92.0V, 2:38 A. M.

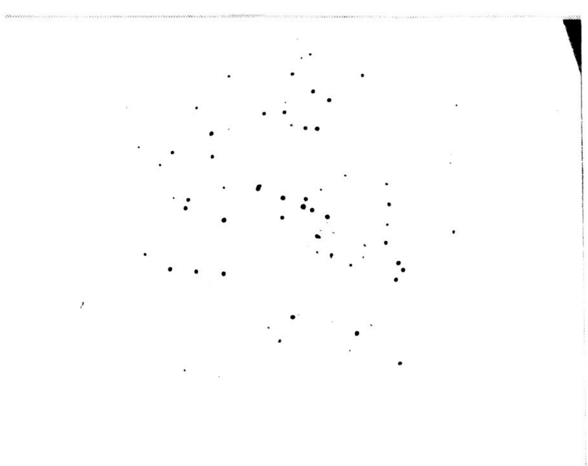

Fig. 46, Orion, 2 sec., 91.6V 2:40 A. M.

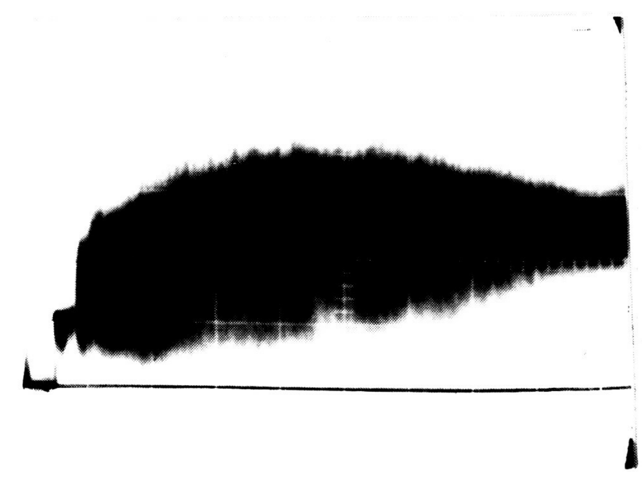

Fig. 47, Range of trace level for one scan.